Memorandum to the DESY-PRC

from the CALICE Collaboration

(CAlorimetry for the LInear Collider Experiment)

The CALICE Collaboration

S.Chekanov, G.Drake, V.Guarino, S.Kuhlmann, S.R.Magill, B.Musgrave, J.Repond, D.Underwood, L.Xia
Argonne National Laboratory

A.Brandt, K.De, C.Hahn, D.Jenkins, V.Kaushik, J.Li, J.Smith, M.Sosebee, A.White, J.Yu
University of Texas at Arlington

G.Blazey, D.Chakraborty, A.Dychkant, A.Maciel, M.Martin, R.McIntosh, V.Rykalin, V.Zutshi
NICADD - North Illinois University, Batavia

C.M.Hawkes, R.J.Staley, N.K.Watson, J.A.Wilson
School of Physics and Astronomy, University of Birmingham

C.G.Ainsley, M.Goodrick, G.Mavromanolakis, M.A.Thomson, D.R.Ward
Cavendish Laboratory, Cambridge University

F.Badaud, G.Bohner, F.Chandez, P.Gay, J.Lecoq, S.Manen, S.Monteil
Laboratoire de Physique Corpusculaire, Clermont

V.Astakhov, S.Golovatyuk, I.Golutvin, A.Malakhov, I.Tyapkin, Y.Zanevski, A.Zintchenko , S.Bazylev, N.Gorbunov, S.Slepnev
Joint Institute for Nuclear Research, Dubna

G.Eigen, E.Garutti, V.Korbel, H.Meyer, R.Poeschl, A.Raspereza, S.Schaetzel, F.Sefkow
DESY, Hamburg

M.Groll, R.-D.Heuer
Hamburg University, Hamburg

E.Norbeck, Y.Onel
University of Iowa

G.Kim, D.-W.Kim, K.Lee, S.Lee
Kangnung National University HEP/PD, Kangnung

M.Faucci Gianelli, B.J.Green, M.G.Green, P.-F.Salvatore
Department of Physics, Royal Holloway, University of London

P.D.Dauncey, C.Fry, D.J.Price, O.Zorba
Department of Physics, Imperial College London

M.Lancaster, M.Postranecky, M.Warren, M.Wing
Department of Physics and Astronomy, University College London

R.J.Barlow, J.Freestone, R.Hughes-Jones, M.Kelly, S.Kolya, S.Snow, R.J.Thompson
The Department of Physics and Astronomy, University of Manchester

N.Shumeiko, A.Litomin, P.Starovoitov, V.Rumiantsev, O.Dvornikov, V.Tchekhovsky, A.Solin, A.Tikhonov
Joint Institute for Nuclear Research, Minsk

F.Corriveau
Department of Physics, McGill University, Montréal

V.Balagura, B.Bobchenko, M.Danilov, R.Mizuk, V.Morgunov, E.Novikov, V.Rusinov, E.Tarkovsky
Institute of Theoretical and Experimental Physic, Moscow

V.Andreev, E.Devitsin, V.Kozlov, P.Smirnov, Y.Soloviev, A.Terkulov
Lebedev Physics Institute, Moscow

P.Buzhan, B.Dolgoshein, A.Ilyin, V.Kaplin, A.Karakash, E.Popova, A.Pleshko
Moscow Engineering and Physics Institute

P.Ermolov, D.Karmanov, M.Merkin, A.Savin, A.Voronin, V.Volkov
Moscow State University

B.Bouquet, J.Fleury, G.Martin, F.Richard, Ch.de la Taille, Z.Zhang
Laboratoire de l'Accélérateur Linéaire, Orsay

M.Anduze, J.Badier, J.-C.Brient, C.Clerc, S.Cholet, F.Gastaldi, G.Gaycken, A.Karar, C.Lo Bianco, P.Mora de Freitas, G.Musat, A.Rouge, J.-Ch.Vanel, H.Videau
LLR - Ecole Polytechnique, Palaiseau

Y.Bonnassieux, P.Roca
Physique des Interfaces et Couches Mince - Ecole Polytechnique, Palaiseau

A.Savoy-Navarro
LPNHE - Université Paris6/7

S.Valkar, J.Zacek
Charles University, Prague

J.Cvach, M.Janata, M.Lokajicek, S.Nemecek, I.Polak, J.Popule, M.Tomasek, P.Sicho, V.Vrba, J.Weichert
Institute of Physics, Academy of Sciences of the Czech Republic, Prague

V.Ammosov, Yu.Arestov, B.Chuiko, V.Ermolaev,V.Gapienko, A.Gerasimov, Y.Gilitski,V.Koreshev, V.Lishin, V.Medvedev, A.Semak, V.Shelekhov, Yu.Sviridov, E.Usenko, V.Zaets, A.Zakharov
Institute of High Energy Physics, Protvino

M.Barbi, G.J.Lolos, Z.Papandreou
Department of Physics, University of Regina

J.Crooks, E.G.Villani, M.Tyndel, R.Turchetta
Rutherford Appleton Laboratory, Didcot

S.W.Nam, I.H.Park, J.Yang
Ewha Woman's University, Seoul

J.Kang, Y.Kwon
Yonsei University, Seoul

I.Kim, T.Lee, J.Park, J.Sung
School of Electric Engineering and Computing Science, Seoul National University

I.Yu
Sungkyunkwan University, Suwon

1 Introduction

The CALICE collaboration is studying the design of calorimetry for the International Linear Collider (ILC). The collaboration has defined an R&D program, specified in the previous submission to the PRC-DESY. It involves two parallel efforts that complement each other. These efforts are to build prototypes of calorimeters with technology envisaged for the ILC and to look at future technical options. The prototype electromagnetic calorimeter (ECAL) is a tungsten-silicon sampling device. The hadronic calorimeter (HCAL) is a sampling calorimeter with steel as radiator, with two possible options for the active detector being considered. One is based on scintillator tiles read through photodetectors and with standard analogue or semi-digital electronic readout, called AHCAL for analogue HCAL. The second uses gas detectors with small pad sizes and digital electronic readout, called DHCAL for Digital HCAL. This document gives the current status of the prototypes as well as on the future technical studies.

Since the last DESY-PRC review of the project, the collaboration has signed a MoA between the institutes which were members at the time of its writing. In addition, the European component of the collaboration applied for funding through an I3-project, EUDET. This has been positively reviewed and the level and direction of funding is currently under negotiation. In addition, it should be noted that new groups from Canada, Korea, the UK, the USA and France have recently joined the collaboration.

2 The Electromagnetic Calorimeter (ECAL)

2.1 Overview

The ECAL prototype under completion is made of 30 readout layers. The structure is built from tungsten wrapped in carbon fibre. The active detectors are silicon diode wafers with a pad size of $1\times1cm^2$. The very front end (VFE) electronics provide preamplification and is located outside of the active area, but on the same PCB as the silicon wafers. This PCB is then connected via cables to VME readout electronics which provide digitization and readout.

A schematic view of the prototype is shown in Figure 2-1, with a different colour used for each of the three stacks of ten layers, where each stack has a different tungsten thickness. This choice ensures a good resolution at low energy, due to the thin tungsten ($0.4X_0$ per layer) in the first stack, and a good containment of the electromagnetic showers, due to tungsten thicknesses two and three times larger in the second and third stacks, respectively. The overall thickness is about 20 cm or $24X_0$ at 90°.
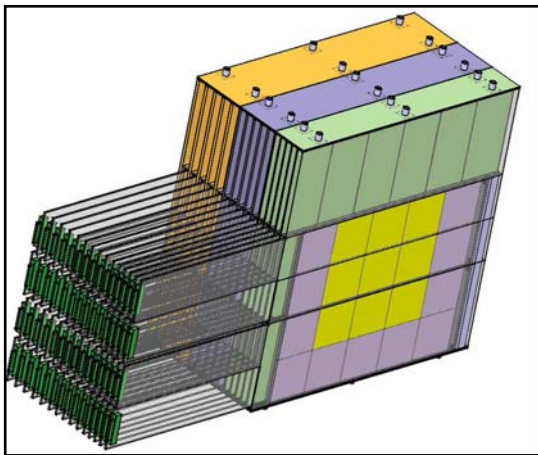

Figure 2-1: Left: Schematic view of the prototype. Right: Photograph of the prototype at the DESY test beam area.

2.2   Mechanical structure

The structure has been constructed by wrapping half of the tungsten sheets in carbon fibre, leaving free spaces (called "alveoli") between each tungsten sheet. Detector slabs are inserted into the alveoli, where each detector slab consists of two active layers and one tungsten sheet. Each active layer is made of a PCB (14 layers, thickness 2.1mm) and up to six high resistivity silicon wafers (thickness 500 μm).

The three stacks of differing thicknesses of tungsten are mechanically separate. All three structures were completed by the LLR group early in 2005 and were using the test beam at DESY (see below) as shown in Figure 2-1.

2.3   Silicon wafer production

The wafers are cut to a size of 62×62 mm^2 which contains an array of 6×6 pads, each 10×10 mm^2, with a space reserved for the guard ring of about 1mm. It should be noted that there is only one set of guard rings per wafer. The wafers are operated in overdepleted mode at a potential of around 200V. The first batch of production wafers, made in Russia by the MSU group, was of very high quality, with a typical leakage current less than a few nA/pad for all the pads, although for a few per cent of the wafers, 1 or 2 pads of the 36 have currents up to 20 nA/pad. These were used to equip the central part of the prototype for the DESY beam tests earlier in 2005 (see below). Because these were the only wafers available, this ECAL test only consisted of around half of the layers, corresponding to about 7 radiation lengths.

The wafer producers perform measurements on the processed wafers before sending them, but the characteristics are not obtain with fully depleted wafers; only one or two pixel are under bias. Therefore, a test stand has been assembled to individually measure the main characteristics of all the wafers (current and capacitance vs. bias) before gluing them onto the PCBs. This measures the same characteristics but with the entire 36 pixel array under bias. For this purpose a wafer mount has been developed which uses conductive foam (allowing I-V measurements) and recently a new system has been made to simultaneously connect to all 36 pixels using spring-loaded metal contact pins (see Figure 2-2), allowing measurements of the I-V curve and capacitance vs. bias (C-V curve) also.
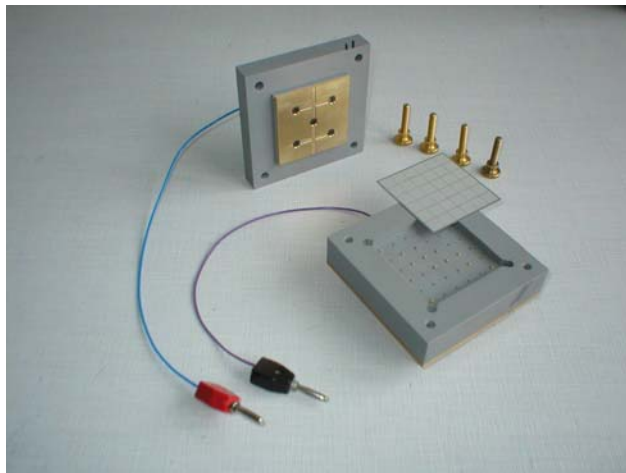
Figure 2-2: New test system with 36 spring-loaded metal contact pins which allows the wafer C-V measurement.

In order to complete the prototype, 96 more wafers are needed to complete the remaining 16 layers of the central part (six of the nine wafers per layer) and 90 wafers are needed for all the layers of the bottom part (three of the nine wafers per layer). Two parallel strategies have been pursued, with wafers ordered both from Elma in Moscow and from ON-Semi in Prague.

2.3.1 Russian wafer production

The total number of processed wafers delivered by MSU and Elma is 145 of the 150 required. Of these 145 wafers, after characterization with the test system, the number of good wafers is 110 (75% of the production). 18 are too close to the requested limits and 17 are bad, either because of a too low breakdown voltage or too high full depletion voltage; see Figure 2-3.
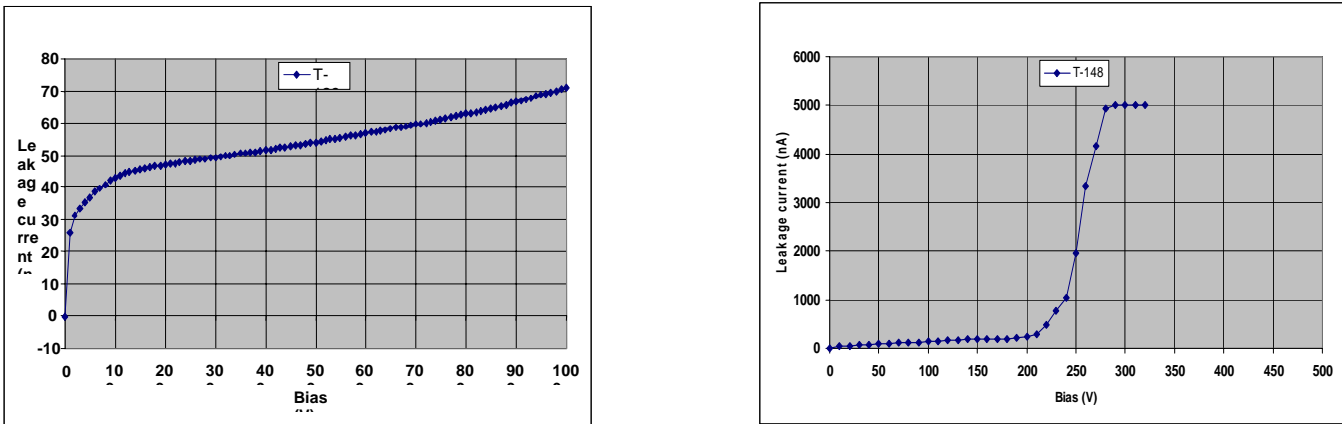
Figure 2-3 Left: Typical I-V curve from good Russian matrix (48 nA @ 200 V, breakdown higher than 1000 V). Right: I-V curve from a bad Russian matrix (breakdown around 220 V).

At the end of March 2005, a further sample of 100 additional wafers were ordered from MSU, in order to at least cover all the central part of the detector. The first 23 wafers were received only in September 2005 and it has been seen that the quality of this first new batch is well below the standard reached during the first wafer production. It seems that less than 65% of the wafers are within specification; 4 wafers show a breakdown voltage which is too small and 8 wafers seems to exhibit a full depletion voltage higher than the 150 V required; see Figure 2-4.

Figure 2-4: $1/C^2$ (proportional to the depletion depth) vs. bias for four Russian wafers received in September 2005. Wafers T-311and T-310 are good as the full depletion occurred lower than 150 V. However, the wafers T-318 and T-320 are not within specification.

2.3.2   Czech wafer production

High quality silicon sensors have been produced in Prague, managed by the Institute of Physics of the Czech Academy of Science. However, problems of compatibility with 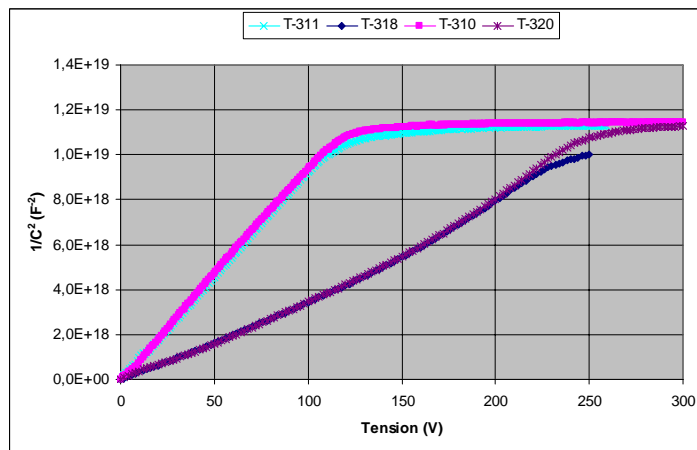the glue used for the electrical contact between the pad and the PCB has been observed. For these wafers, the glue vapour released during the processing at high temperature attacks the passivation layer on top of the wafer, leading to a rising leakage current as a function of time (typically over a period of a few days after gluing, as shown in Figure 2-5).
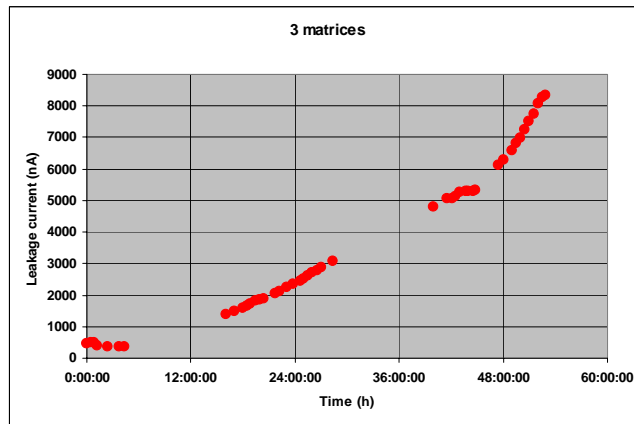
Figure 2-5: I-V curve as a function of time for wafers with glue problem

In April 2005, with the people from Institute of Physics of Prague, a new gluing protocol has been tested with a higher curing temperature and shorter heating time. The results of these various tests were not very conclusive but it appears that the wafers already manufactured cannot be recovered. It clearly became imperative to make another production with a significant change to the passivation layer and possibly to the guard ring also. ON-Semi, the Czech company, therefore changed the passive layer on the top of wafers, in order to be compatible with the gluing. In August 2005, 10 new processed wafers were received. Measurement done before gluing on all 10 wafers shows result in agreement with specifications, but after gluing just two wafers, a large increase of the leakage current (ten times higher than before gluing) is observed. However, unlike the first wafers produced by ON-semi, the breakdown voltage seems to be stable (see Figure 2-6). Other tests are under investigation and new result will be available in few weeks.

Figure 2-6: I-V curves before (blue) and after (yellow) gluing for Czech wafer T-019-19, received in August 2005.

2.4   Readout electronics

2.4.1   The very front end electronics

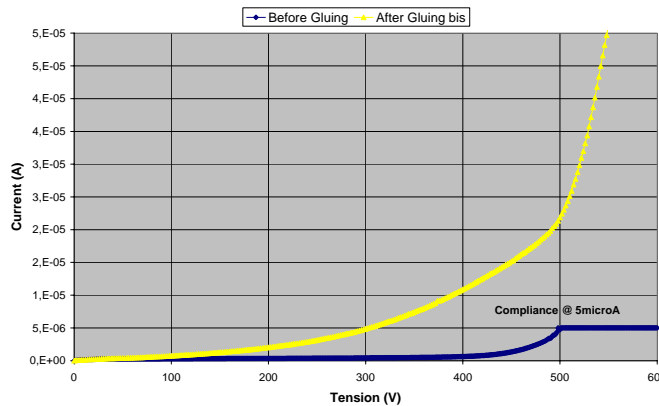The silicon wafer diodes are read by a VFE chip developed by the LAL-Orsay group. It consists of a preamplifier with two gains, a shaper and a multiplexer. This chip handles 18 channels and has low noise and a large dynamic range. The latest version, FLC_PHY3 [1], is used for the ECAL prototype. The PCB has been designed at LAL-Orsay and has been produced in Korea under the control of KNU. All VFE chips and PCBs required for the ECAL have been fabricated and are in hand.

2.4.2   The VME electronics

The hardware to read out the front end electronics is the CALICE Readout Card (CRC) [2]. This is a custom-designed 9U VME board, developed from the CMS silicon tracker readout. It contains 16bit, 500kHz ADCs for digitisation and an 8MByte buffer for data storage during a spill. CRCs will be used to read out the ECAL, AHCAL and TCMT, as well as provide a VME control for the trigger. All data from these detectors can be digitised and stored in less than 100μs after the trigger. Each CRC can handle up to 1728 channels and the total system (ECAL, AHCAL, TCMT and trigger) will require 13 CRCs, spread over two VME crates.

At the time of the last PRC, two prototype boards had been produced. Since that time, the prototype board were tested successfully with only minor modifications needed for the production version. Two production CRCs were then fabricated in November 2004 and used for the cosmics and beam runs between December 2004 and February 2005. A further seven production boards were then assembled in March 2005 and have been fully tested. All nine existing production CRCs are now characterised and functional. A further seven CRCs have been ordered through Rutherford Laboratory to complete the system. These are due for delivery in November 2005. Testing should take three to four weeks.

The main outstanding issues for the CRCs are with the firmware. Two major upgrades will be needed to achieve the requirements. The first is to handle the data from the trigger itself; currently these can only be read via a slow serial path and this would limit the trigger rate within the spill. The second is to increase the usuable amount of the on-board buffer; currently only 2MBytes of the 8MBytes total is accessible and only 500 events can be stored. Both these improvements are under development and should be implemented by early 2006.

The other hardware needed for the DAQ is mainly in hand. The two 9U VME crates have been in use at DESY throughout 2005 and the final VME readout system and online disk array were purchased in April 2005. The major remaining item is the cables, which are common to the ECAL and AHCAL, and these are scheduled for purchase in early 2006.

2.5   First results in 2005

The partially completed ECAL was exposed to cosmics for a short period in December 2004 and January 2005 and this was followed by a run at the DESY test beam in January and February 2005.

2.5.1   Cosmic tests

The cosmic test bench at LLR was used to take over 1×10^6 events during a two week period through Christmas and New Year in 2004/5. The system was left running unattended throughout this time, demonstrating the stability of both the calorimeter and the DAQ system.

From the cosmics data a signal-over-noise ratio of 8 was obtained, as shown in Figure 2-7. The fraction of cells with a higher noise level was below 0.3%. No sign of coherent noise was seen; at most 0.7ADC (3% of the most

probable (MPV) MIP signal) of noise is due to coherent noise on the whole PCB, which contains 216 channels. This level would cause a measurement error on the signal of 3% in the worst case in which all pads have a signal just above the hit threshold (~40% of the MIP MPV). In the general case, in which larger signals (much greater than 1 MIP) are concentrated on a few pads, the error is much smaller. The raw dispersion of the signal response is of the order of 3%. However, the cosmics data were used to calibrate the individual cells to a level of 1%.
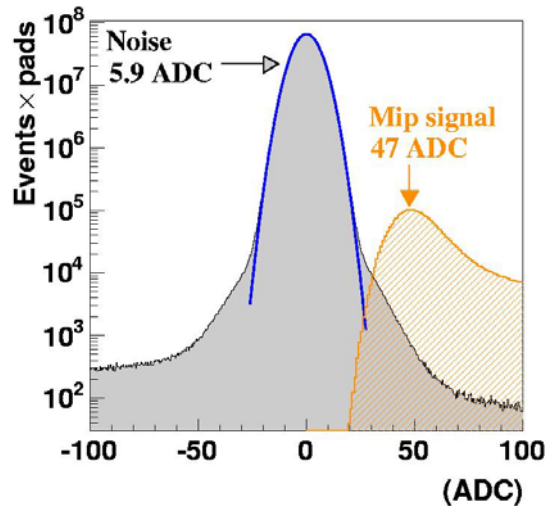

Figure 2-7: Measurement of the MIP signal and the noise level from the cosmics data.

2.5.2   Test in beam at DESY

A first test of the Si/W ECAL prototype was performed at DESY with electrons during January-February 2005. The structure consisted of 14 tungsten layers; the first 10 were 1.4 mm thick each and the last 4 were 2.8 mm. Each was interleaved with an 18×12 matrix of active silicon wafer cells, each 1×1 cm². In total, the detector had 3024 channels, corresponding to about $7.2X_0$ at normal incidence.

The test beam layout is shown in Figure 2-8. Three scintillation counters were used to provide the trigger signal and there were four drift chambers which perform the tracking of the incoming particles. The calorimeter prototype was put on top of a movable table to allow horizontal and vertical displacement with respect to beam. Data at several configurations of position, energy and angle were taken. Position scans were performed at the centre, edges and corners of wafers, with the electron beam energy mainly at 1, 2, 3 GeV, although some runs at 4, 5 and 6 GeV were also take. Data were take with normal incidence and with the detector tilted with respect to the beam direction up to 30°. In total about $25×10^6$ trigger events were recorded.
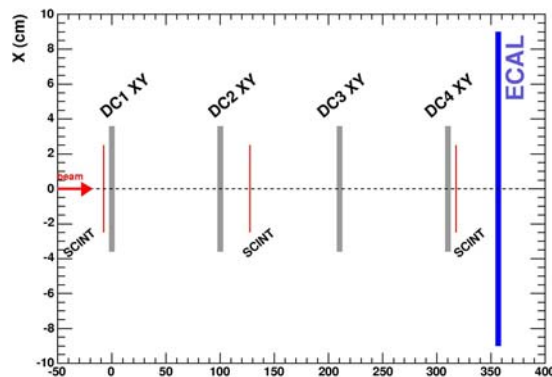

Figure 2-8: Layout of the test beam taken at DESY

A typical event is displayed in Figure 2-9, where cells with a signal hit above a threshold of 0.5 MIP are shown. This illustrates clearly the concept of "tracking calorimetry"; the high granularity of the calorimeter allows a record of the development of the shower along both transverse and longitudinal directions. It can be reconstructed in a tracking manner, i.e. both calorimetric and tracking information are provided. A close up view of a very interesting event is also shown in the same figure, where two electrons reach the prototype simultaneously
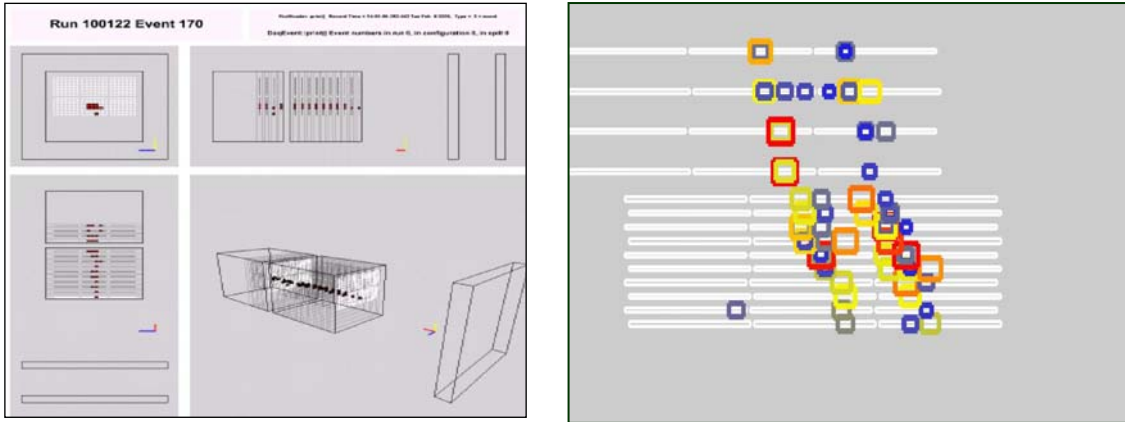
Figure 2-9: Left: Display of a typical event. Right: Interaction of two close electrons in the same event.

The first analysis of the test beam data gave a thorough understanding and allowed for significant debugging of the system. Further systematic analyses are in progress, such as studies on position resolution, tracking performance, response variations, inhomogeneity, transverse shower containment, Moliere radius, etc.

An example of some results with respect to position resolution and transverse containment studies are shown in Figure 2-10. They illustrate the excellent tracking capabilities of the detector and the narrow transverse size of the shower expected, due to the high granularity of the calorimeter and the tungsten absorber, respectively.

Figure 2-10: Left: Position resolution as a function of the electron beam energy. Right: Fraction of shower energy contained within cylinder of given radius around the shower axis.

Despite being limited by the small depth of the calorimeter used, the results from these studies are useful for planning and guiding the next test beam phase. Although they are not conclusive at this stage they are indicative of detector characteristics. The current series of studies will serve as reference analyses to be repeated as detector grows and new data come.

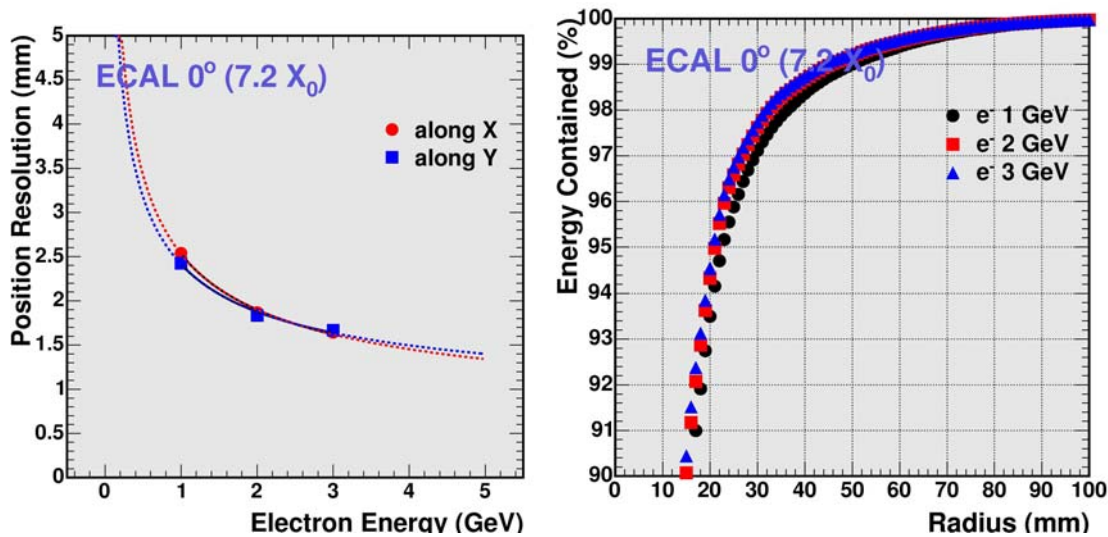By the end of this year more layers will be added to the prototype detector to reach a full depth of about $24X_0$. This will allow full containment of electron showers and thus more conclusive studies with respect to energy, angular and position resolution of the calorimeter can be performed. In particular, the major aim is a more detailed comparison with the performance expected from the GEANT4 simulation.

To conclude, this test beam period has been very successful for checking the performance of the detector and the readout and for a first round of analysis.

2.6   Silicon-tungsten ECAL long-term R&D

R&D on the technology for the full scale ILC detector is progressing in several different directions.

- Two new VFE chips will be produced in 2006. The goal is the design and test of a new VFE chip type post-prototype. This is in progress at LAL-Orsay, LPC and LPSC with production of an ASIC called FLC-TECH1, which will include built-in ADC(s) and will work in pulsed mode. One of the goals is to validate the simulation of the chip, which predicts a power dissipation (in pulsed mode) of about 100 µW/channel, to test the level of noise when the ADC is included, etc.

- Thermal simulations at MSU, LLR, Manchester and KNU have begun to see the impact of the geometry, material used, etc. The goal is to validate designs regarding the power dissipation.

- A review is underway of possibilities for on-detector readout electronics for final project, where available space is very small. It includes a study of "improved" zero suppression at the digital level for an ECAL module.

- The study of the new design has started, where the readout electronics is placed within the calorimeter active area. This results in the VFE chip being mounted on a backside of the PCB which has the wafers glued on the other side. The overall thickness per layer is smaller (giving a good Moliere radius) and the serial noise is reduced. A test PCB has been produced and is shown on Figure 2-11.

- Studies of on-off detector data transfer and off-detector receivers have been started in the UK. These aim for a backplaneless architecture based on commercially available hardware rather than custom designs.

- A conceptual study into the use of monolithic active pixel sensors (MAPS) for the ECAL sensitive layers has begun in the UK. This study aims to produce two prototype sensors over the next few years to compare their performance with the baseline silicon diode pad designs. This includes a possible beam test with a few layers of MAPS sensors in 2008.
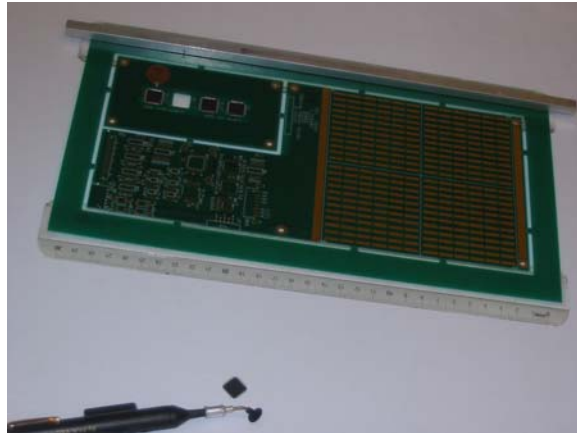
Figure 2-11: A PCB of the new design, with readout ASICs attached to the back of the wafer PCB.

2.7   Conclusions

The ECAL prototype is aiming for completion of the central part of all 30 layers with an expected deadline around January 2006. Test beam at DESY would then allow the first test of the prototype with full thickness. Following completion of the remaining bottom parts of the layers, a period of test beam with high energy electrons and hadrons is then foreseen at CERN in the second part of 2006 followed by a run at FNAL in 2007.

3   The Digital Hadron Calorimeter (DHCAL)

3.1   Overview

The purpose of this project is to develop a Digital Hadron Calorimeter (DHCAL) for the Linear Collider detector. A calorimeter optimized for the application of Particle Flow Algorithms (PFLOWs) features a very fine segmentation of the readout, of the order of 1 cm^2 laterally and layer-by-layer longitudinally, for both the electromagnetic and the hadronic parts of the calorimeter. With this fine segmentation, the energy resolution for neutral hadrons (the component of hadronic jets to be measured with the HCAL) obtained with digital or analog readout is comparable.

Two different choices for the active medium of a DHCAL are being considered: Gas Electron Multipliers (GEMs) and Resistive Plate Chambers (RPCs). GEMs are being studied by groups at University of Texas at Arlington, the University of Washington, Tsinghua University, and Changwon National University. RPCs are being investigated by a group in Russia (IHEP Protvino and Dubna) and, independently, by a group in North America (Argonne, Boston, Chicago, FNAL, Iowa and Regina). In comparison, GEMs offer the advantage of lower operating voltages (hundreds of volts compared to several thousand volts for RPCs) and RPCs offer easier assembly techniques, mechanical robustness and larger electronic signals (several pC compared to several fC). A choice between the two technologies will be based on a comparison of their performance as active medium of a prototype calorimeter section in test beams.

The goal of the project is to build chambers to fully equip a 1 m^3 prototype section of a hadron calorimeter. The section will contain 40 active layers each with an area of about 1 m^2. The chambers will be designed such that they can be used together with the mechanical structure now being assembled for the AHCAL.

3.2   Recent Progress

In the following we shall briefly summarize recent progress of the different subprojects and their plans for the next few months.

3.2.1   Gas Electron Multipliers

The group has been developing the implementation of the DHCAL using GEM technology [3]. The ionization signal from charged tracks passing through the drift section of the active layer is amplified using double GEM foils. The amplified charge is collected at the anode, or readout pad, layer, which is at ground potential. This layer is subdivided into the small ($\sim 1 \times 1 cm^2$) pads needed to implement the digital approach.

The potential differences, required to guide the ionization, are produced by a resistor network, with successive connections to the cathode, both sides of each GEM foil, and the anode layer. The pad signals are amplified, discriminated, and a digital output produced. The GEM design allows a high degree of flexibility with, for instance, possibilities for microstrips for precision tracking layer(s), variable pad sizes, and optional ganging of pads for coarser granularity future readout if required by cost considerations. Figure 3-1 shows how the GEM approach is incorporated into a digital calorimeter scheme.

Previously we reported initial results on signal characteristics and gain from a small prototype GEM detector. The signals from the chamber are being read out using the QPA02 chip developed by FNAL for silicon strip detectors. The gain of the chamber was determined to be of the order of 3.5×10^3, which is consistent with measurements done on similar chambers by the CERN GDD group. The MIP efficiency was measured to be 94.6% for a 40mV threshold, which agrees with a simulation of chamber performance. The corresponding hit multiplicity for the same threshold was measured to be 1.27, which will be beneficial for track following and cluster definition in a final calorimeter system. A gas mixture of 80% Ar/20% CO_2 has been shown to work well, and give an increase in gain of a factor of 3 over the original 70% Ar/30% CO_2 mixture. A minimum MIP signal size of 10 fC, and an average size of 50 fC derive from the use of this new mixture. The prototype system has proved very stable in operation over many months, even after deliberate disassembly and rebuilding – always returning to the same measured characteristics.

Here we give an update of results from the past year. These have been collected using the detector shown in Figure 3-1 using the anode pad layout shown in the same figure.
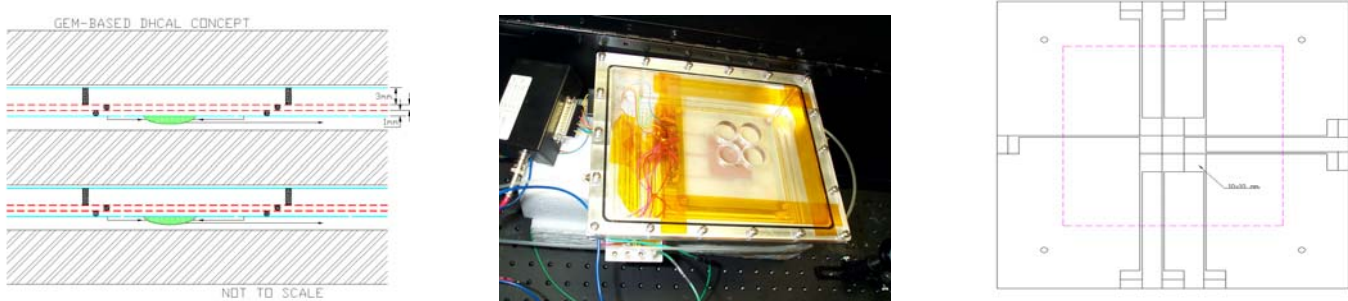

Figure 3-1 Left: GEM-based digital calorimeter stack. Centre: Prototype GEM detector. Right: Nine pad anode layer.

Using multi-pad readout we have studied the crosstalk between neighbouring cells. A typical (but rarely occurring) situation is shown in Figure 3-2. The large peak is the signal on the central pad of the 3×3 arrangement. The up-

down peaks of the second trace are the crosstalk signal on an adjacent pad. We have reproduced these peaks using direct signal generator pulse injection. The results are shown in the same figure. We have also used collimated gamma rays from a Cs^{137} source to study signal sharing between adjacent pads. A typical sharing of signals between pads is also shown in Figure 3-2. Note the absence of a "down" peak as seen for a crosstalk signal.
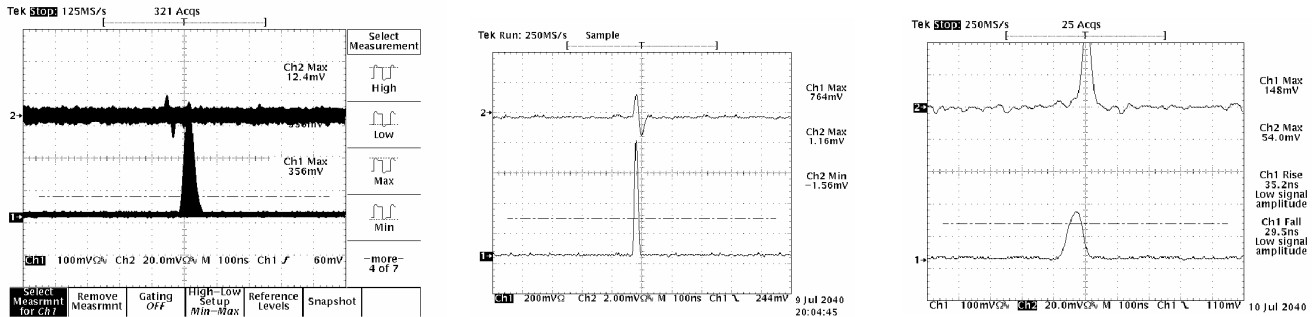

Figure 3-2 Left: GEM crosstalk signal. Centre: Generation of crosstalk. Right: Observed signal.

The group have also looked into the effects of changing the proportion of Argon in our Argon-CO_2 gas mixture. We find that we obtain a factor of three increase in signal size changing from a 70/30 mixture to an 80/20 mixture. The latter mixture has given very stable detector performance over weeks of operation with no discharges. We therefore expect minimum signal sizes for MIPs in the10 fC range using the 80/20 mixture; minimum signals in this range ease the design of the front-end ASIC described below.

For the full-size test beam module, and final elements of a GEM-based DHCAL system, we are targeting ~1m×30cm detector panels. We have been working in two main areas: the mechanical aspects of large GEM-layer assembly, and the fabrication of large area GEM foils. The layer assembly has required development of tools to hand large area foils, and present them flat for integration into a detector. We have also developed initial components for the detector walls (1mm and 3mm heights are required), gas in/outlets, and spacers to maintain the separation of the foils. Further valuable information will be learned in the assembly of 30×30cm^2 detectors. A roll of eighty 30×30cm^2 foils has been produced by 3M and is being evaluated. Figure 3-3 shows the 3M GEM foil mass production facility, one of the new 30×30cm^2 foils and a large test GEM mechanical assembly which is close to its completion.
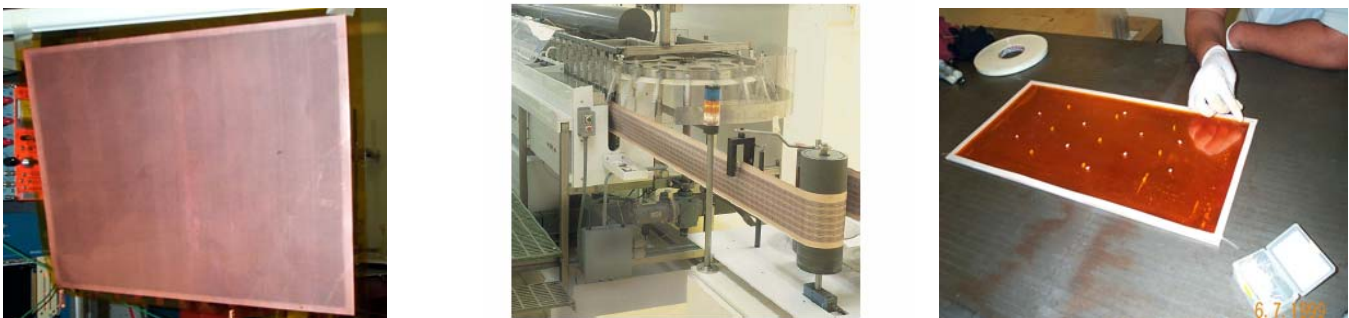

Figure 3-3: Left: A 3M GEM foil roll production facility. Centre: New 30×30cm^2 GEM foils produced by 3M. Right: Large area mechanical prototype.

These foils will also be evaluated by the other member institutions of the GEM/DHCAL group, and by U. Victoria and Louisiana Tech. University for ILC tracking applications. As an intermediate step, five double-GEM chambers are being constructed using the $30 \times 30 \text{cm}^2$ foils. Each chamber will have a $10 \times 10 \text{cm}^2$ active area, giving a total system of 500 channels. This system will be used to repeat efficiency, hit multiplicity, and crosstalk measurements. The readout system is being designed by U. Washington and will likely use electronics developed for the BES muon system.

As the first step toward large scale GEM detector development, we will construct a stack of five double-GEM 30cm $30 \times 30 \text{cm}^2$ detectors. We plan on using three of the 32-channel FNAL preamp cards, already used for our earlier prototype, as the front-end readout. We will read out a central area of 96 channels per detector, as shown in Figure 3-4.
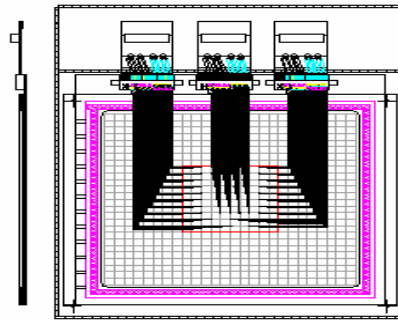

Figure 3-4 Schematic of anode layer and front end electronics for the multi-channel prototype.

As reported above, we have been using 32-channel FNAL QPA02 ASIC card to test prototype double GEM detectors at UTA for some time. A total of 15 cards are needed to readout the 500 channels of the cosmic ray stack and will be mounted directly on to each layer of the stack. FNAL has assembled enough cards for us using the existing QPA02 chips. The output signals from the amplifier cards will be sent to discriminator boards which contain discriminator chips, multiplexer stages and data output interface. The output from the discriminator boards will be readout by a DAQ card in a PC controlled by LabView. The discriminator boards and DAQ system will be developed at the University of Washington.

The stack will be used to examine the following items: single cosmic tracks hit patterns, hit multiplicity (vs. simulation), signal sharing between pads (e.g. vs. angle), efficiencies of single DGEM counters, effects of layer separators, operational experience with ~500 channel system, as a possible test-bed for an ASIC when available (rebuilding one or more DGEM chambers).

The principal tasks for the next three years will be the construction and testing of a full size (1m^3) GEM-based digital hadron calorimeter stack with a total of 40 longitudinal layers. This is an essential step in the development of linear collider detector technology, in order to (a) demonstrate the viability of this technique (in parallel with the scintillator and RPC-based approaches), and (b) make critical, energy density measurements with fine granularity ($\sim 1 \times 1 \text{cm}^2$), to tune GEANT4 as a reliable tool for PFLOW development. The test beam stack will be built at UTA using the 1m×30cm GEM foils. There will thus be three double GEM panels for each of the forty $1 \times 1 \text{m}^2$ layers.

The UTA group has successfully implemented a double GEM layer geometry into the existing Mokka code [5], a GEANT4 [6] based simulation package, replacing the scintillation counter sensitive layers in the TESLA TDR hadronic geometry (stainless steel/ scintillation counter) with the detailed double GEM layer structure. All other detector structures were kept the same as in the TESLA TDR detector design [7]. In order to optimize computer CPU resources, a simplified version of the GEM was implemented instead of detailed geometry. A comparison using single 75 GeV pion events shows virtually identical energy deposits in half the CPU time for the simplified mixture version compared to a detailed geometry of a double GEM structure. Based on this study, we have decided to use the simplified geometry for further studies.

Using the established simulation and analysis software, we have completed the study of double GEM-based calorimeter performances in analogue and digital readout modes with a realistic threshold value at 98% of a MIP, using single pion samples whose energies range from 5 GeV to 100 GeV. The intrinsic gain of the double GEM sensitive layers was chosen to be 3000, the value measured from our prototype, which is within 15% of other measurements. The results from these studies have been compared to TESLA TDR detector performance studies based on Mokka. The resolution obtained from our studies of TESLA TDR detector is consistent with results from other studies, if an energy-independent electromagnetic and hadronic relative normalization factor of 0.65 is used.

The group used the same data set generated for the analogue studies of GEM calorimeter to perform digital studies. Figure 3-5 shows a profile plot of E vs.N for hit-to-energy-deposit conversion. The same figure also shows the scatter plot of energy vs. number of hits, which demonstrates the linearity of the detector in its digital readout mode. As expected saturation in the number of cells hit begins to appear at the higher energy deposits due to larger energy densities in a cell. It has been observed in our study that 85% of the cells are hit once for 5 GeV single pion showers while this fraction decreases to 74% for 100 GeV single pion showers. A study of number of hit cell vs. layer number for 50 GeV pion shows that it directly mimics the energy deposit distribution along the layer, providing direct evidence and confidence that a GEM based calorimeter can be used as a digital calorimeter properly representing energy deposit of showers. We used the number of hit cells versus energy deposit to extract the hit-to-energy-deposit conversion factor for digital readout mode analysis.
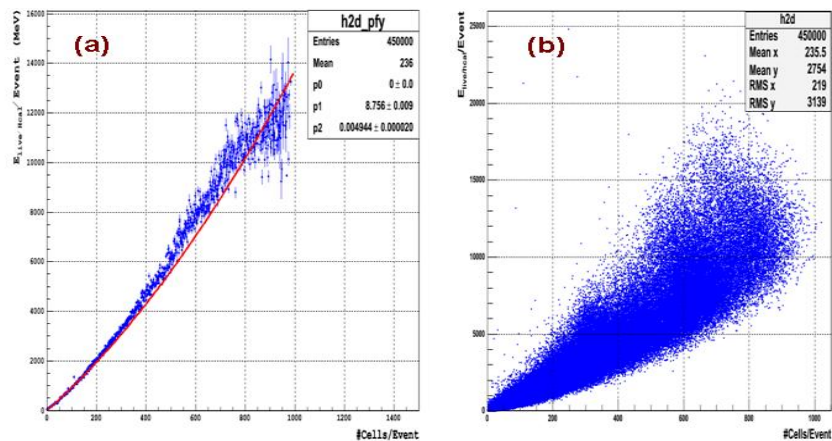

Figure 3-5: Left: A profile plot of energy deposit vs. number of cells hit used for hit-to-energy-deposit conversion. Right: Scatter plot of energy deposited. A saturation at the higher energy deposit is seen.

A more sophisticated procedure for fitting the responses from EM and hadronic components had to be developed to accommodate the changes in energy deposit distributions for analogue and digital modes. The energy deposit measured in analogue mode shows a remaining large tail due to Landau fluctuations. These large fluctuations are suppressed in digital mode since the tail of higher energy deposits within a cell are still counted as one hit forcing the distribution Gaussian. Figure 3-6 shows distributions of energy deposits by 50 GeV pions for analogue and digital modes, respectively. The arrows indicate the threshold and the corresponding efficiency. From this study we find that 0.23 MeV for muon energy deposit gives 95% MIP efficiency. The performance of GEM DHCAL with thresholds has been completed without incorporating realistic noise measurements. The above studies of GEM DHCAL performance were carried out by two Master's students. The results from the data analysis have been documented in S.Habib's [8] and V.Kaushik's Master's theses [9].
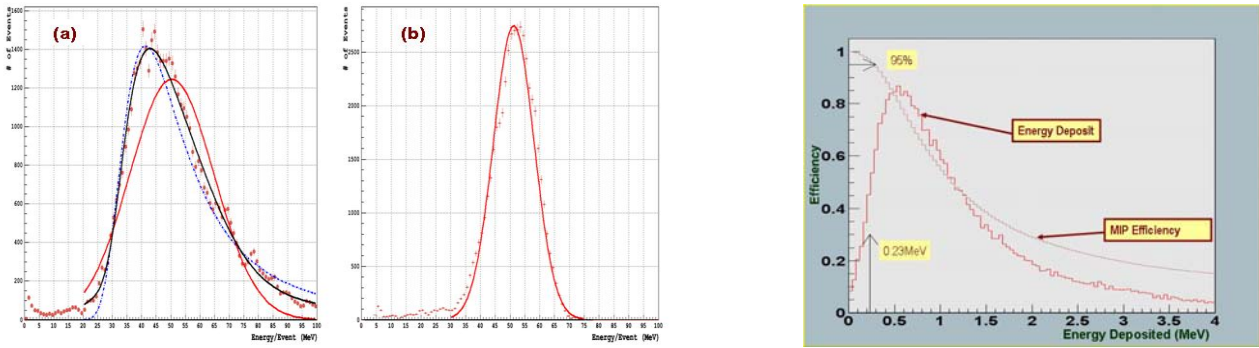
Figure 3-6: Left: Energy deposit of 50 GeV pions (red circles) in GEM DHCAL (a) in analog and (b) in digital modes. Right: Energy deposit of a 50 GeV muon in the GEM calorimeter (red histogram) and the MIP efficiency as a function of discriminator threshold (dark red).

Performance studies show that GEM calorimeter responses for analogue and digital are very closed to each other as we expected. The resolution curves of TESLA TDR detector in analogue readout mode and GEM calorimeter in analogue and digital modes with a 98% threshold are shown in Figure 3-7. The single pion energy resolution of the GEM digital calorimeter is comparable to that of TESLA TDR and other detector studies for most the energy ranges except at low energies. This is reflected in the resolution function as the digital mode showing larger sampling terms (~70%) with relatively smaller constant term. On the other hand, the GEM analog mode resolution is significantly worse than other detectors or than the digital modes. This behavior is caused by the large remaining Landau fluctuation in energy deposit as discussed above.
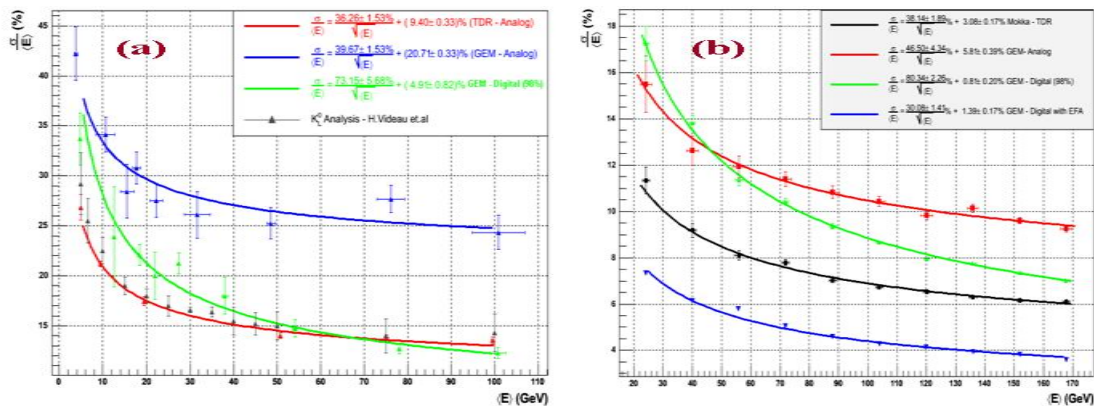

Figure 3-7 Left: Energy resolution for TESLA TDR (red), GEM analogue (blue), GEM digital (green) modes and other detectors (triangles). Right: Jet energy resolutions using various detector techniques. The blue line represents the GEM digital with PFLOW.

Once the final single particle energy resolution is known, it is straightforward to apply these functions to smear particles in a jet to test the performance of PFLOW and the given calorimeter technology. We used Pythia to generate $t\bar{t}$ to 6 jet events to test the performance. In order to carry out the study, we had to define a "jet" in simulated events. In the absence of an official applicable jet algorithm, we took a simple cone algorithm of size $\Delta R=0.5$ around the direction of the final state parton to define a particle jet. We then took each particle and smeared its energy using the parameters of single particle resolution functions, and add all smeared particle energies inside the cone for measured jet energies. This procedure is slightly changed for PFLOW jet energy resolution. We smeared the energies of all charged particles by an expected tracker momentum resolution, $\Delta p/p = 10^{-5}$, and all

electromagnetic particles, including hardons whose final states are EM particles, such as π^0 and η^0, with an EM calorimeter resolution, $15\%/\sqrt{E}$. As shown in Figure 3-7, PFLOW based jet energy resolution using GEM DHCAL (blue line) demonstrates the best resolution with the sampling term at around 30% which is consistent with the expectation.

Improvement in jet energy resolution can be obtained using the energy flow algorithm. For PFLOW to work, one of the most important procedures is the subtraction of calorimeter energies that correspond to charged tracks whose momenta are measured in the tracking system. Since any algorithm of such subtraction must work very efficiently in simple cases, we have carried out a preliminary PFLOW studies in two step process. First we determine the best algorithm to identify the centroid of a hadronic shower using single pion events. We explored three distinct methods for centroid determination. The three methods are: (a) energy weighted method, (b) simple averaging and (c) density weighted method. A study shows that while all three methods seem to perform well, density weighted method seems to perform the best for digital methods. We then proceed to two pion shower cases in a GEM based detector in its digital mode using full detector simulation in Mokka through multiple iterations of matching calorimeter and tracker positions to draw the cone of size ΔR=0.1 (half the distance between any two particles).

A study in detector granularity for GEM detector will be conducted to determine cell sizes that can be accommodated without compromising PFLOW performance of the detector. This will also be the same for other parameters, such as absorber thickness, sensitive gap size, on-board readout electronics sizes, and mechanical support structures. This will be carried out as part of the recently initiated LC detector initiatives in both the silicon detector (Si-Detector) and the Large Detector concepts.

The current level of PFLOW development is very rudimentary since the clustering algorithms for associating the track with the corresponding shower is simply a cone drawn around the centroid of the shower [9]. Given the erratic behavior of hadron showers, the algorithm should be more flexible in its areas of subtraction of shower energies. We will work closely with Argonne National Laboratory and other groups in PFLOW development. Once a reasonably performing algorithm has been developed, we will move on to a multi-jet environment to test performance of the algorithm.

Since the hardware development effort will move onto constructing a 30×30cm^2 five layer cosmic-ray stack and taking data, it is necessary to have software and simulation evolve to support this activity. In order to compare the performance of the cosmic-ray stack with expectations from simulation, the new geometry needs to be implemented in the simulation package. In addition, cosmic-ray data analysis software must also be developed. The data from the cosmic-ray stack and the simulation can then be used for development of tracking algorithms through the calorimeter. These studies will need to be done in both analog and digital modes to compare performances. In addition, a study on E vs. B field impact to the incident charged particles, causing the particles to spiral in the gas gap. The geometry for GEM foils has been implemented for Maxwell simulation. The GEM geometry has also been integrated into the SiD detector concept studies for the studies of performances in a more integrated detector structure.

We expect to participate in a test beam experiment [10] on the 2006 – 2008 time scale, contingent upon availability of funds. The geometry for test beam experiment must be implemented and the corresponding software for reconstruction and analysis must be developed ahead of the actual data taking. Currently, Northern Illinois University and SLAC have developed a test beam simulation package. We plan to exploit the existing package and implement our GEM geometry into the system for the initial studies in the test beam stack, along with utilizing Mokka.

3.2.2   Resistive Plate Chambers (Russia)

The group carried out an extensive study of the performance of mono-gap glass RPC prototypes with 1×1cm^2 anode readout pads. The RPC prototypes were operated in saturated avalanche and in streamer mode. In both modes the chambers showed excellent detection efficiency (>95%) and low pad multiplicity (<1.4) for single tracks.

Comparing the two operation modes, the group concludes that the saturated avalanche mode is to be preferred, mostly due to its higher rate capability and safer operation mode. Overall, the chambers meet the requirements on the performance of the active medium of a digital hadron calorimeter for the Linear Collider, as determined by simulation studies.

As a result of our studies, the group recommends the use of RPCs with the following features:

- Single-gap chambers (for simplicity reasons),

- Thin glass sheets as resistive plates (commercially available),

- Gas gaps of 1.2 – 1.6 mm thickness,

- Resistive anode plates as thin as possible,

- Anode pads with a size of about 1 cm^2,

- Operation in saturated avalanche mode,

- Use of the following gas mixture: TFE/IB/SF_6, with 5% isobutane and a few % SF_6,

- Signal discrimination at about 2 mV (for 50 Ω loads).

Further details have been documented in [XXX] the publication "RPC as a Detector for High Granularity Digital Hadron Calorimetry", DESY-04-057 (March 2004).

A 1 m^2 RPC prototype plane was constructed for use in the 1 m^3 DHCAL prototype section. The chamber rests on a 2 mm steel sheet which provides the necessary rigidity of the structure. The uniformity of the response was measured with cosmic rays using 2 x 16 orthogonal x and y readout strips, each with an area of 96×6 cm^2. A MIP detection efficiency of 95% was measured with a uniformity of ±2%. The chamber performed satisfactorily for the use in the 1 m^3 prototype section and can, if needed, be produced in the required quantity.

RPC prototypes with 64 pads of 1×1 cm^2 were assembled to be tested in a 5T magnetic field at DESY, oriented perpendicular or at 45° relative to the electric field. The chambers are readout with the 8-channel Minsk chips together with ALTERA FPGAs. Two such prototypes were successfully tested with cosmic rays. No influence of the magnetic field on the RPC performance was found.

In preparation for beam tests of RPC planes with 32×32=1024 channels different versions of the anode pad printed board (to transfer signals to the side of the module) were build and evaluated. In all cases the pad multiplicity was observed to be higher than with cable connections and not satisfactory. It was therefore decided to use anode pad boards with 50 Ω cable connections to the FE PCBs. The FEE PCBs have been fabricated and the assembly is in progress. In addition, a new RPC plane was constructed. Beam tests of this RPC plane with 1024 channels is expected in Nov-Dec. 2005 at IHEP.

3.2.3   Resistive Plate Chambers (US)

The group assembled a total of ten Resistive Plate Chambers, nine with an area of 20×20 cm^2 and one with an area of 91×32 cm^2. Three of these chambers feature double gas gaps, whereas the remainder features single gas gaps. All chambers use glass with a typical thickness of 1.2 mm as resistive plates. A photograph of one of the chambers is shown in Figure 3-8.
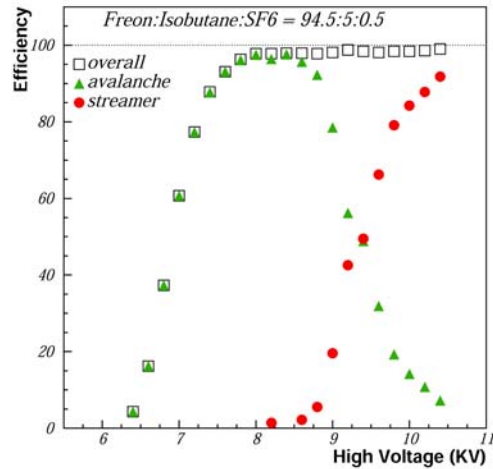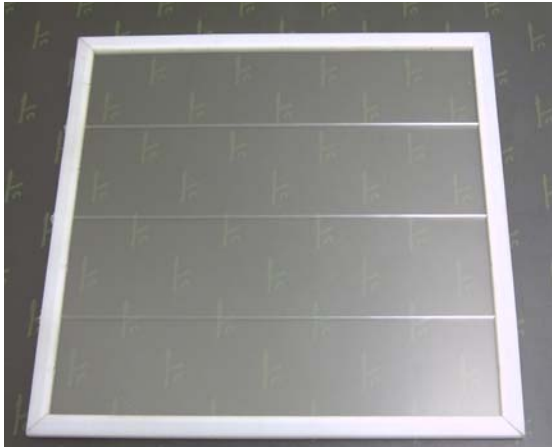

Figure 3-8 Left: Photograph of a resistive plate chamber with an area of 20×20 cm^2. Right: Single pad MIP detection efficiency and streamer fraction as function of applied high voltage

In one chamber the readout pad face the gas volume directly, without an interleaved glass plate. The chambers were thoroughly tested with cosmic rays and sources. The analogue measurements were performed using the RABBIT system developed for CDF and the digital measurements used a VME based digital readout system developed and built by this group. In the following we briefly summarize the many tests performed with the chambers:

- The MIP detection efficiency of the chambers, the charge of the signals and the streamer fraction were measured as function of applied high voltage with a single readout pad of 10 x 10 cm^2 and analog readout.

- The MIP detection efficiency and the noise rate were measured as a function of applied high voltage with a single readout pad of 10 x 10 cm^2 and digital readout (amplifier and discriminator). The results are shown in Figure 3-8.

- The above measurements were repeated with a number of different gas mixtures.

- The geometrical acceptance of the chambers was measured using a cosmic ray test stand with tracking capability.

- Measurements were performed with multiple pads: 64 pads of 1 cm^2 each. The MIP detection efficiency and the pad multiplicity were measured as a function of applied high voltage with both analogue and digital readout. The results are shown in Figure 3-9.

- The mechanical properties of the chambers under gas pressure and as a function of applied high voltage were determined. Figure 3-10 shows the deflection at the centre of a 91 x 32 cm^2 chamber as function of pressure. The pressure was applied uniformly by pouring water on the glass surface.

- The rate capability of the chambers was measured using a source for irradiation and cosmic rays to determine the MIP detection efficiency. The measured MIP detection efficiency as function of instantaneous rate is also shown in Figure 3-10.
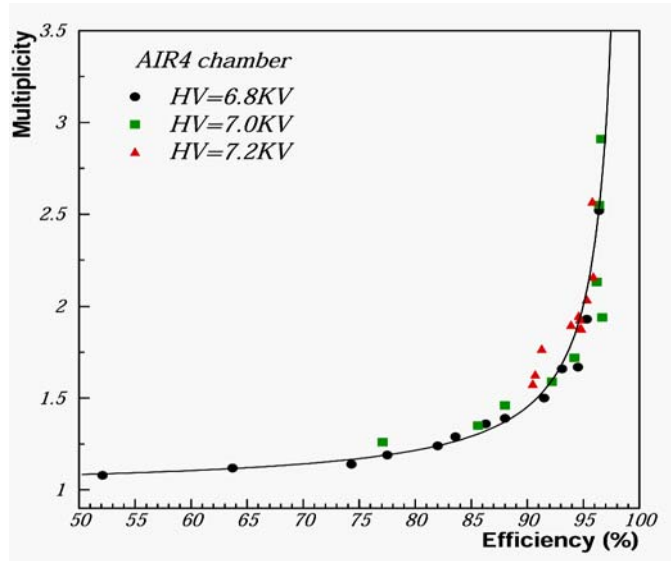

Figure 3-9: Pad multiplicity versus MIP detection efficiency for three different high voltage settings. For a given high voltage, the detection efficiency was varied by adjusting the discriminator threshold.

From these tests we conclude that RPCs are an excellent candidate for the active medium of a digital hadron calorimeter: the MIP detection efficiency is high (> 95%), the noise rate is extremely small (< 0.5 Hz/cm^2), the pad multiplicity is of the order of 1.5 to 1.6 (with digital readout), and the chambers can handle rates of at least 50 Hz/cm^2 without loss of efficiency.

A RPC design for the prototype section has been developed. In the next few months we plan construct and test a prototype chamber based on our default design for the 1 m^3 stack.
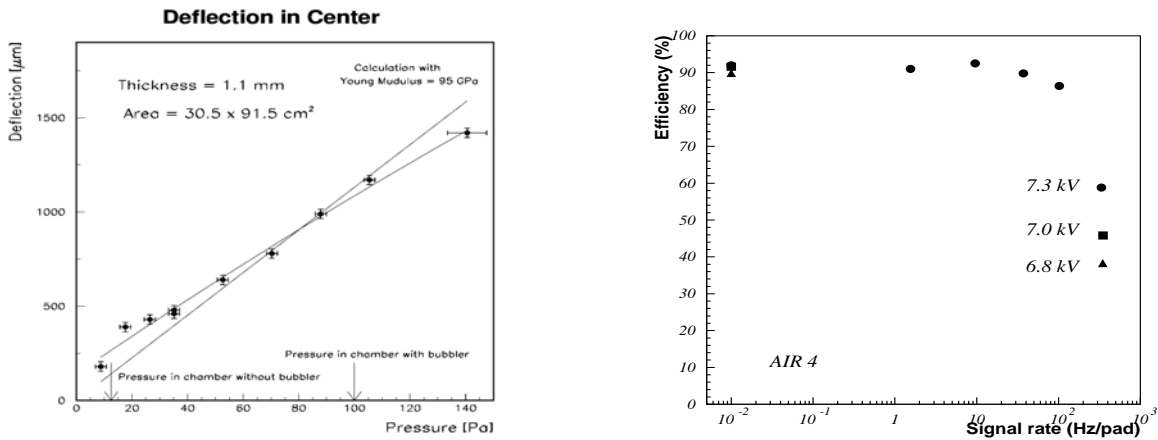

Figure 3-10: Left: Deflection measured at the centre of a 30.5 x 91.5 cm^2 glass plate. The gas pressure resulting from a "bubbler" at the outlet is indicated with an arrow. Right: MIP detection efficiency as a function of instantaneous rate for three different high voltage settings.

3.3   Readout electronics

The group developed a conceptual design of the electronic readout system for the prototype section. The system consists of several parts: front-end ASICs, front-end readout-boards, data concentrator boards, super concentrator boards, data collection system and trigger and timing modules. A block diagram of the system is shown in Figure 3-11. In the following we shall briefly describe the major parts of the system and the status of their development.

3.3.1   Front-end ASIC

Each front-end ASIC is connected to 64 readout pads. The input signals are amplified and passed through discriminators, providing a hit pattern together with a 24-bit time stamp. The chip can operate in both triggerless and triggered mode. The chip design is complete and a first prototype has been produced and is being evaluated. A photograph of a prototype ASIC mounted on a test board is shown in Figure 3-12.

3.3.2   Front-end readout boards

The front-end readout boards cover an area of 48×32 cm^2 and contain 1536 readout pads connected to 24 front-end ASICs. The boards will contain both analogue and digital lines. A test board to measure the cross-talk between the analogue and digital lines has been fabricated. First measurements indicate the need for a carefully designed grounding strategy.
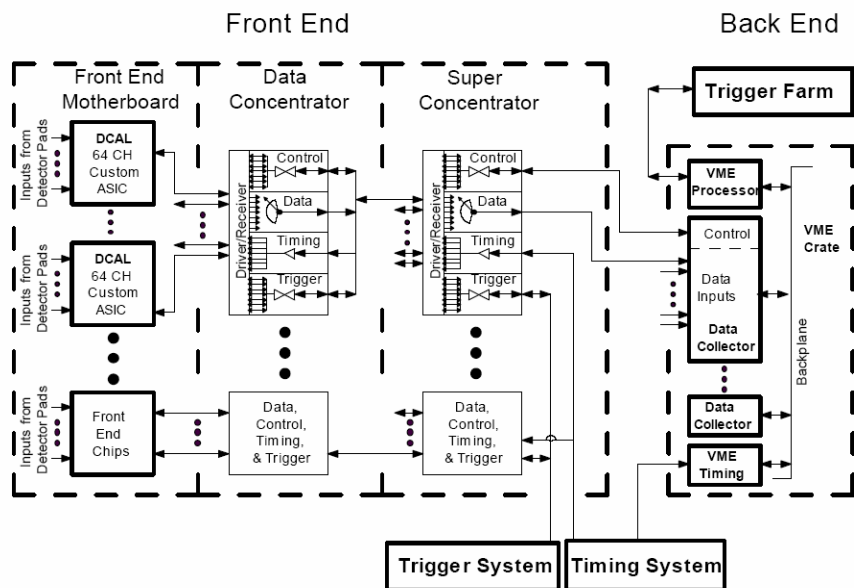

Figure 3-11: Block diagram of the electronic readout system for the DHCAL prototype section.
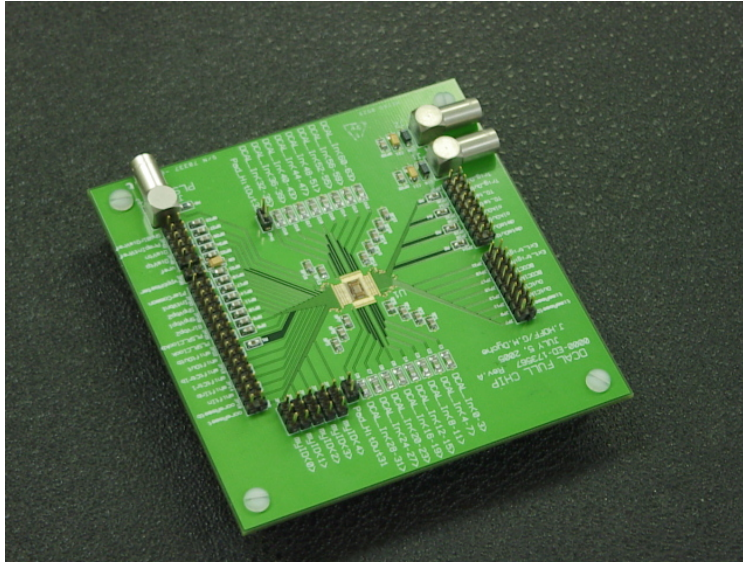
Figure 3-12: Photograph of prototype front-end ASIC mounted on a test board.

3.3.3   Data Concentrator boards

These boards will be located on the side of the 1m^3 stack and read out 12 ASICs each. In addition, the boards will distribute the slow control signals and clocks to the front end.

3.3.4   Super concentrator board

Further multiplexing is provided by the super concentrator boards. Each board will connect to six data concentrators and, thus, readout half a plane of the 1 m^3 stack. Their architecture will be similar to the data concentrator boards and be centred on an FPGA.

3.3.5   Data collector

The back-end of the system will most likely be based on VME and consist of seven cards in a 9U crate.

Despite the difficult financial situation, the group will proceed with the detailed design and prototyping of the various parts of the electronic readout system. Final designs are expected to be available sometime during the first part of 2006. At which time construction of the electronics for the 1 m^3 prototype section may start, provided the necessary funds have been secured.

3.4   <u>Summary</u>

RPCs have been proven to perform adequately for the use in a hadron calorimeter with digital (1-bit) readout. Specific recommendations concerning the details of the chamber design have been made for use in a 1 m^3 prototype section. In addition, the development of GEMs as the active medium is progressing well towards a full test beam stack.

The development of the electronic readout system is also progressing well. A document describing the conceptual design of the system has been produced. The design of the individual parts has commenced. In particular the design of the front-end ASIC is complete and first prototypes are now being tested.

Contingent on the availability of adequate funding, construction of the RPCs and GEMs and the corresponding readout system for the prototype section will start in calendar year 2006. Tests in particle beams will initiate in calendar year 2007.

4   The Analogue Hadron Calorimeter (AHCAL)

4.1   Overview

With the advent of the silicon photomultiplier (SiPM), a Geiger mode solid state photodetector, at moderate cost, high longitudinal and lateral readout granularities can be realized with scintillators. The scintillator-based AHCAL development is pursued as an option for an imaging hadron calorimeter, which holds the promise of meeting the demands [11] on spatial and energy resolution imposed by the PFLOW detector concept for linear collider physics.

The goals of the AHCAL project are twofold: on the technology side, the aim is to gain large-scale, long-term experience with a SiPM readout detector and to identify critical operational aspects for further system optimization. On the physics side, the purpose is to collect the large data samples (order of 10^8 events) needed to explore hadron showers with unprecedented granularity, validate hadronic shower simulation models and develop energy weighting and PFLOW reconstruction algorithms. Due to the current large model dependence of predictions for PFLOW-relevant shower properties [12] it is indispensable to base the final detector optimization on real beam data. In that respect the term "prototype" may be misleading: the aim is a "proof of principle". Technical solutions scalable to a full detector design are only partially addressed and will be a subject for future R&D.

The basic tile size of the prototype was optimized with respect to particle separation capability [13] and found to be $3\times3\times0.5$ cm^3. Such a small size is also suggested within the semi-digital approach [14] where one chooses a moderate granularity (relative to the 1 cm^2 pad size proposed for the gaseous digital option) in conjunction with a two-bit, three-threshold readout. The prototype calorimeter will allow tests of both the analogue and the semi-digital HCAL options with a single device.

In order to save channel count and cost, the high granularity is restricted to a 30 layer, 30×30 cm^2 core, resulting in 216 channels for each of the first 30 layers. This core is surrounded by larger (6×6 and 12×12 cm^2) tiles, resulting in a total number of channels of around 8000 for all 38 layers. This step of two orders of magnitude with respect to the 99-channel Minical (see Section 4.2) represents a tremendous challenge for the industrialization of SiPM production and quality control (see Section 4.3) as well as for the scintillator tile plus WLS. It also demanded a new integrated front end electronics concept for the readout in the combined (ECAL and AHCAL) beam test and for the individual SiPM bias voltage adjustment (see Section 4.5). A versatile calibration and monitoring system [15] (see Section 4.6) and a modular mechanical design (see Section 4.4) were required in addition.

This challenge is being met by a collaborative R&D effort with a rather high degree of task sharing; for an overview see Table 1. For such a distributed effort a well structured software environment is essential. This is being developed [16] on the basis of the inter-regional LCIO data model in close interaction with the ILC simulations and software group (see Section 6).

Table 4.1 Task sharing in the tile HCAL test beam prototype effort

SiPM production and tests	MEPhI, ITEP
SiPM tile systems	ITEP
Module construction, LED light distribution	DESY
LED calibration electronics	Prague
Front end ASICs	LAL
Front end boards	DESY
DAQ	Imperial College, Manchester, RAL, UCL
Absorber stack, movable table, slow control	DESY
Commissioning	DESY, Hamburg, MEPhI, later NIU, all

4.2   Experience with the Minical

The SiPM [17] is a pixelated avalanche photodiode which provides a gain of $\sim 10^6$, comparable to that of vacuum phototubes. On a 1 mm^2 surface 1024 pixels operate independently in limited Geiger mode and produce a signal corresponding to the number of fired pixels. Due to its small size, high gain, low bias voltage (typically 50 V) and insensitivity to magnetic fields (tested up to 5 T [18]), the device can be mounted directly on scintillator tiles for individual readout.

Only very recently have SiPMs become available from Russian industry in larger quantities. First experience with a 99 channel AHCAL prototype ("Minical") was gained in 2003 in the DESY positron test beam and was reported to the PRC in spring 2004. Final results have meanwhile been published [18]. The Minical is a sandwich structure with 2 cm steel absorber plates interleaved with 11 active layers, each containing 9 scintillator tiles ($5 \times 5 \times 0.5$ cm^3) with SiPMs mounted directly on the tile and collecting the light via a circular wavelength shifting (WLS) fibre. The light yield of this tile fibre SiPM system was 25 ± 5 pixels per minimum ionizing particle (MIP).

The limited number of pixels on a SiPM introduces noticeable non-linear effects; for 6 GeV electromagnetic showers the energy depositions in the shower core ranged up to an equivalent of almost 100 MIPs per tile, with mean values up to 40 MIPs. The effects could successfully be corrected on a channel-by-channel basis using a single well-measured SiPM response function together with the measured light yield (LY) in terms of pixels per MIP for individual tiles. The LY calibration requires the observation of single photo-electron signals, for which special front end electronics was connected. Figure 4-1 shows the measured energy and resolution as a function of beam energy. The uncorrected data (open circles) demonstrate the size of the non-linearity correction for the entire shower. The results compare well with those obtained with conventional multi-anode vacuum phototubes and with APDs (not shown here; see [19]). They are well reproduced by a Monte Carlo simulation which includes the detailed SiPM behaviour. Thus, after correction the saturation effects do not degrade the calorimeter linearity and resolution. The successful Minical experience encouraged the group to proceed towards the construction of a cubic-meter sized prototype for hadron beam tests, based on SiPMs.
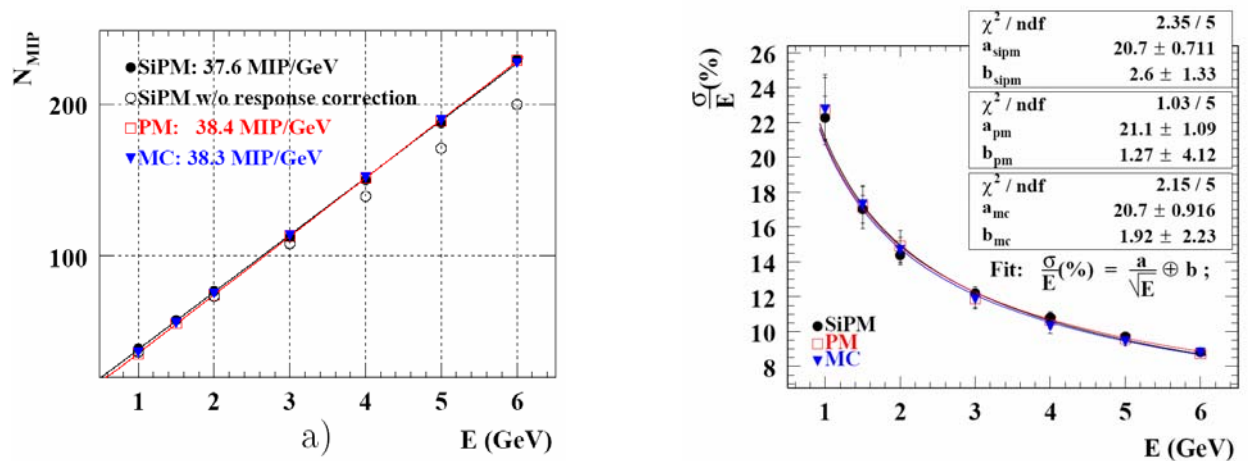
Figure 4-1: Left: Minical linearity with and without the response correction. Right: Minical resolution vs.incident electron beam energy.

4.3 Overview

4.4 SiPMs and scintillators

Mass production of SiPMs is still a pioneering endeavour, led by the PULSAR company in close cooperation with MEPhI. A first attempt to produce the quantity needed for the prototype failed; the performance was too much degraded due to insufficient wafer quality. A second attempt was more successful and has a yield which should provide sensors for about half the prototype. Production of the remainder is still the source of some schedule risk.

The properties of the SiPMs for the prototype are the same as in the Minical, except for the choice of a larger value for the quenching resistor (around 10 MΩ instead of 400 kΩ). This improves the pixel uniformity and reduces the sensitivity to the exact calibration light pulse duration, since it results in a longer pixel recovery time.
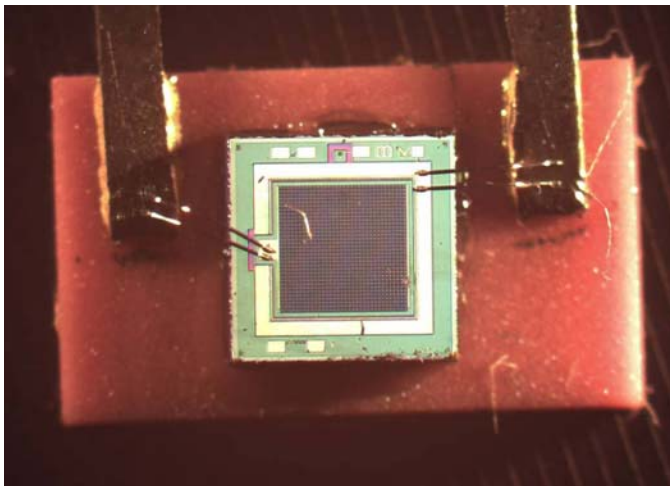

Figure 4-2: Left: SiPM on a support plate. Right: SiPM inserted into a 3×3cm^2 tile.

Quality control proceeds in several semi-automatic steps. While the basic functionality (sensitivity to visible light at an acceptable dark current) can be first checked on the un-cut wafer in a probe station at the production site, the determination of the proper bias voltage working point and of the parameters for the final selection can be done only after mounting the sensors on their support plate (see Figure 4-2). For this second step, the detectors are transferred to a dedicated test bench at ITEP. The third stage (also at ITEP) is the determination of the actual light yield after assembly of the tile-fibre-SiPM system. After this procedure each system comes with its own complete data sheet which contains all parameters from dark rate to response function and is stored in a data base. As an example, two parameters (dark noise rate and inter-pixel cross-talk) are shown in Figure 4-3 for a sample of about 2500 tested SiPMs. These two parameters determine the noise rate above a given threshold, say 0.5 MIP. For the selected SiPMs and nominal light yield, this rate corresponds to about one spurious hit per event in the prototype. In practice the occupancy is higher, since for tiles with smaller light yield the threshold has to be lowered.
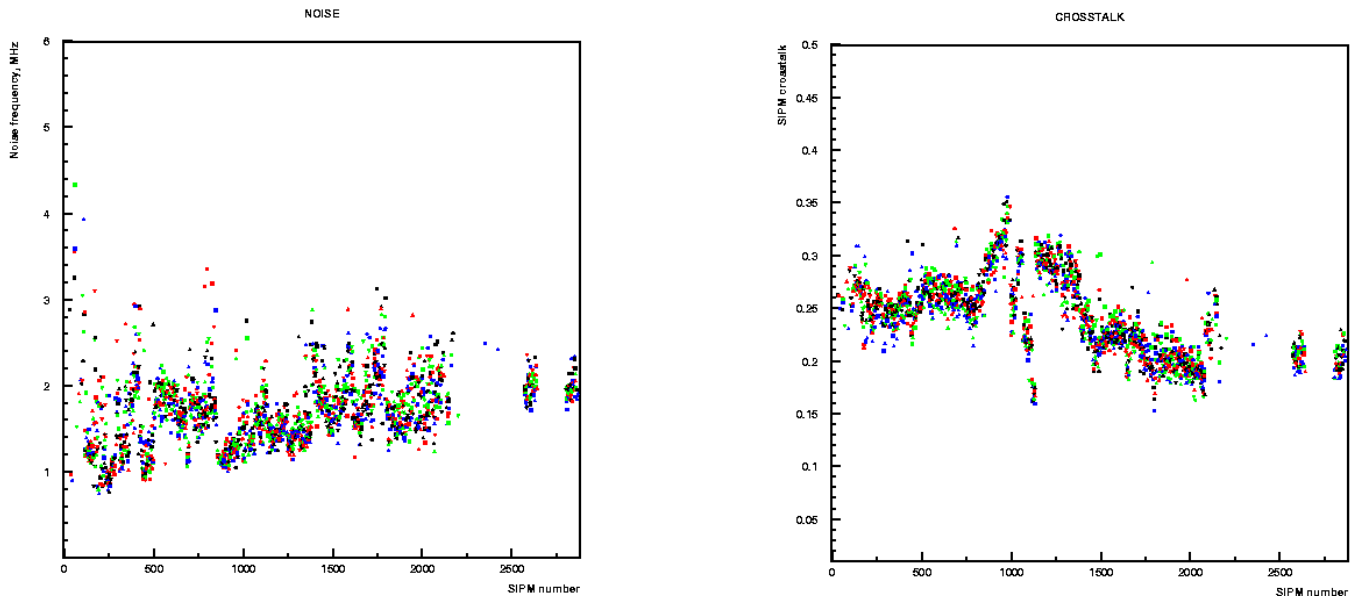

Figure 4-3: Left: SiPM dark noise rate vs. sensor serial number. Right: SiPM inter-pixel cross-talk at the selected bias voltage vs. sensor serial number.

About 10% of the SiPMs installed in the first two modules exhibited an overly high noise rate due to long discharge pulses, with a higher occurrence where the bias voltage had been increased by up to 5V. The phenomenon had not been observed in the Minical, and only occasionally on the test bench. In detailed investigations this was correlated to defects of the aluminium microstructure on the SiPM surface which deteriorate the quenching resistor of more or more pixels. This is thought to originate from production or assembly steps. SiPMs produced for later assembled modules are equipped with a surface-protecting layer, but these have not been tested in modules yet. In the meantime, the quality control measures have been upgraded and include day-long simultaneous tests of 240 SiPMs operated at increased bias voltage. The result of these measures will be known in the forthcoming weeks.

Until recently, the Minical represented the world stock of SiPMs. After the test beam run some of the sensors were used for long-term studies. No parameter variations were seen, albeit with limited statistics. This important issue will be re-addressed while the detector modules are being commissioned.

Scintillator production has been completed to a large extent. A 3×3 cm^2 tile type is shown in Figure 4-2. The tile edges have been matted by chemical treatment for diffuse internal reflection and suppression of optical cross-talk between adjacent tiles, which is then limited to < 2%. The light yield is presently adjusted to be 15 ± 1.5 pixels per MIP, a compromise between MIP signal-to-noise separation and dynamic range.

4.5   Module construction and the mechanical structure

At the time of this review, about 1300 tiles for the first 6 layers have been assembled and tested at Moscow, and shipped to DESY. Figure 4-4 shows the tile array laid out in the steel cassette. The size of the active area is 90×90 cm^2. In the next step of module assembly, the tiles are covered with a plastic (FR4) board which serves as a support for calibration light fibres and for the 1 mm micro-coax readout cables, which are connected to the SiPMs via small flexible PCBs. A fully assembled module with front end electronics connected is also shown in Figure 4-4.

Figure 4-4: Left: Scintillator tile layer. Right: Complete module with front end electronics.

The complete module will be inserted into the absorber stack structure, of which the parts have been constructed, and which is shown mounted on top of a moving stage in the design drawing of Figure 4-5. The drawing shows the configuration set up for inclined beam incidence; the construction ensures that the beam still passes through the high granularity core in all layers for angles up to 35°. The stack and its support have been designed in a modular and flexible way which allows it to be adapted for beam tests with other active modules, for example with resistive plate chambers for tests of the DHCAL. Integration of the set-up into the test beam environments at FNAL and CERN is under study now. The steel absorber has not been designed for operation inside strong magnets; the effects of magnetic fields on shower development and reconstruction must be studied in simulation.
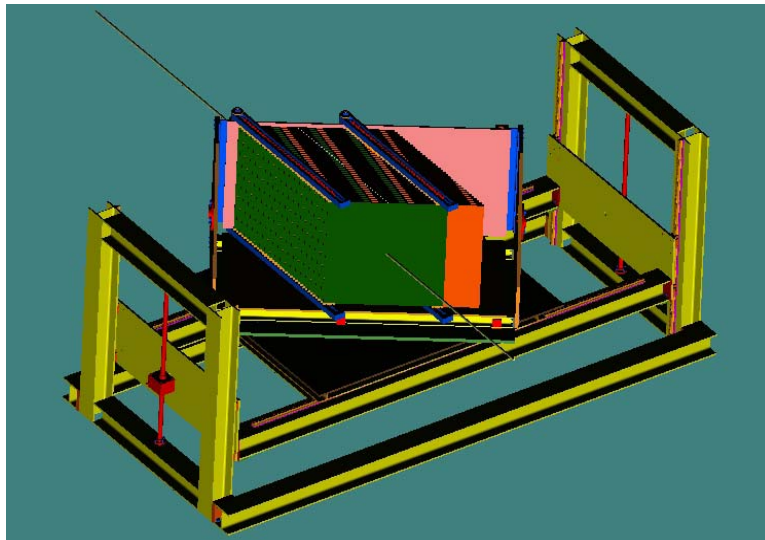

Figure 4-5: HCAL absorber stack on its movable table.

4.6   Readout electronics

The AHCAL prototype has a similar number of analogue readout channels as the CALICE silicon tungsten ECAL prototype, which both eventually have to be integrated in a combined test beam setup. The AHCAL readout concept was therefore based on the same architecture, using the same back-end data acquisition and adapting the front-end electronics to the SiPM needs. The ECAL front-end consists of an 18-fold multiplexed pre-amplifier and shaper with a sample-and-hold in a single ASIC, FLC-PHY3 [1], and is followed by the VME back-end CALICE readout cards (CRC) [2] with 8 input ports, each port receiving the signals from 12 ASICs on 16-bit ADCs. The CRCs can run at more than 1 kHz instantaneous input rate, have sufficient on-board memory to buffer 2000 events and can process the data at an average event output rate of 100 Hz.

A new ASIC chip, ILC-SiPM, was developed, prototyped and produced in less than one year and is presented in more detail in [20]. The ASIC contains for each of its 18 channels an 8-bit DAC for adjustment of the SiPM bias voltage in a 0-5 V range and thus solves the problem of supplying 8000 different and adjustable operation voltages to the calorimeter prototype.

As there is no pipeline, the maximum trigger latency time is determined by the peaking time of the front-end shaper of about 180 ns. With such a long shaping time, the observation of single pixel SiPM signals is hampered by pile-up of noise signals occurring at a rate of 2-3 MHz. Thus, for calibration purposes, the preamplifier-shaper must switch to shorter peaking time and larger gain; for LED pulses trigger latency is not an issue. The new ILC-SiPM chip has a high degree of configurability of shaping parameters; see the block diagram in Figure 4-6. The figure also shows a SiPM pulse height spectrum with well distinguishable single-pixel signals, recorded with the ILC-SiPM.
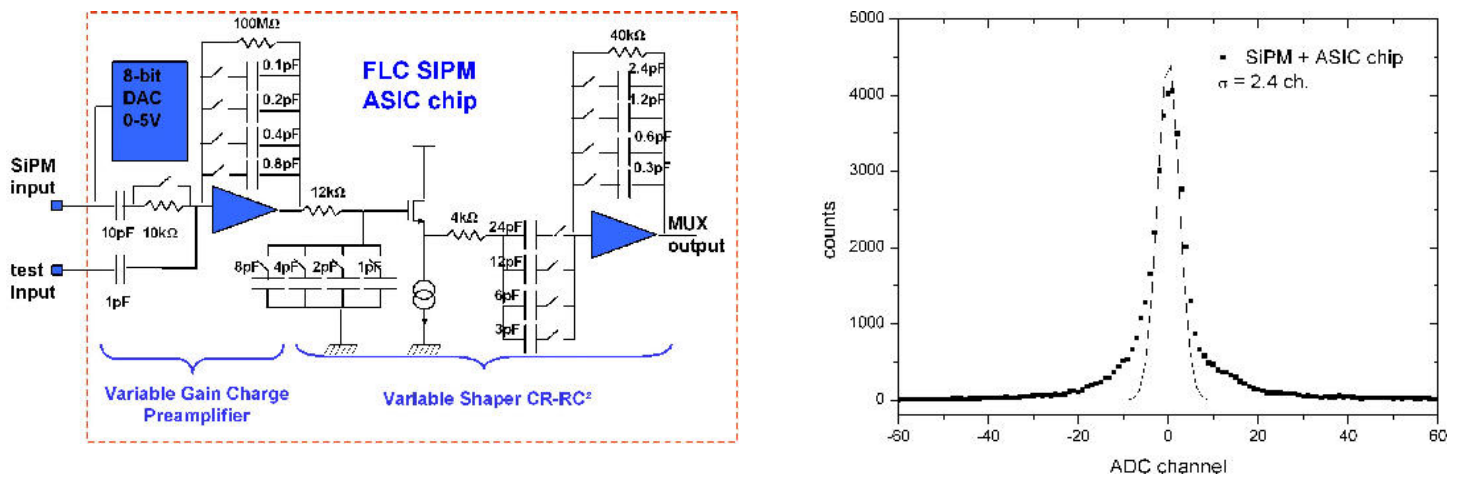

Figure 4-6: Left: ILC-SiPM block diagram. Right: ILC-SiPM random trigger signal ("pedestal") with electronics contribution (SiPM bias off).

The front end electronics are realised as a baseboard plus piggy-backs, as shown in Figure 4-4. The piggy-backs each hold one ASIC and the shift registers for its configuration, while the base boards provide the connection to the SiPMs on one side and the interface to DAQ and power supplies on the other. The layout of the signal lines ensures timing uniformity at the ns level which is critical for the fast-shaping calibration mode, as there is only one adjustable delay per AHCAL layer. One AHCAL module can thus be connected to one CRC port, the whole prototype can be read out with five VME boards in one crate. The same components (ASIC and boards) will also be used for the TCMT, which is also read out with SiPMs. Production and testing of all ASICs (LAL) and FE boards (DESY) for the test beam prototype have been finished on schedule with high yield.

An alternative electronics and DAQ concept, based on fast digitisation, has been developed by the Dubna group and can be tested on an assembled AHCAL module.

4.7 Calibration and monitoring system

The non-linearity of the SiPM response poses unusual demands on the calibration system. It is foreseen to use the procedures established in the Minical. However, with the short Minical test beam runs it had not yet been necessary to seriously address the issue of stability and monitoring. Since the SiPM response varies with temperature, additional measures must be taken to ensure optimal physics performance over longer run periods. A redundant calibration and monitoring system [8] is foreseen, which injects the light from 12 LEDs per layer into each tile via individual clear fibres. The intensity of each LED is monitored with a PIN photo-diode.

The LY calibration requires collecting a high statistics sample of MIP like events. This can be achieved using cosmic muons, a broad muon beam or a broad hadron beam obtained from a metal brick installed in front of the calorimeter to initiate hadronic showers. In all these cases the calibration takes several hours and cannot be used to monitor the system stability. The other ingredient for the LY calibration, illustrated in Figure 4-7, is the SiPM gain which is obtained from the separation between two neighbouring single pixel peaks when the SiPM is illuminated with low intensity LED light. Assuming a DAQ rate limit of 100 Hz, it takes about 20 min to collect 10^5 events, yielding a precision of 1-2% for the gain determination. In order to collect these data simultaneously for all channels, the spread in light intensity injected from a single LED into the 18 tiles must not be too large. This required a careful optimization of the light distribution system (Figure 4-8).
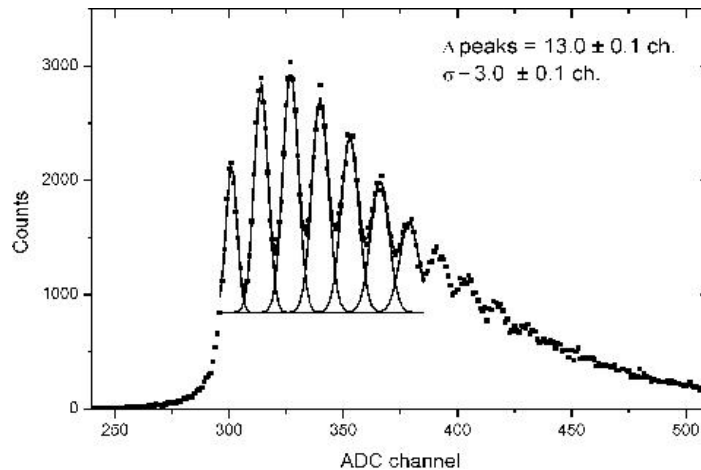

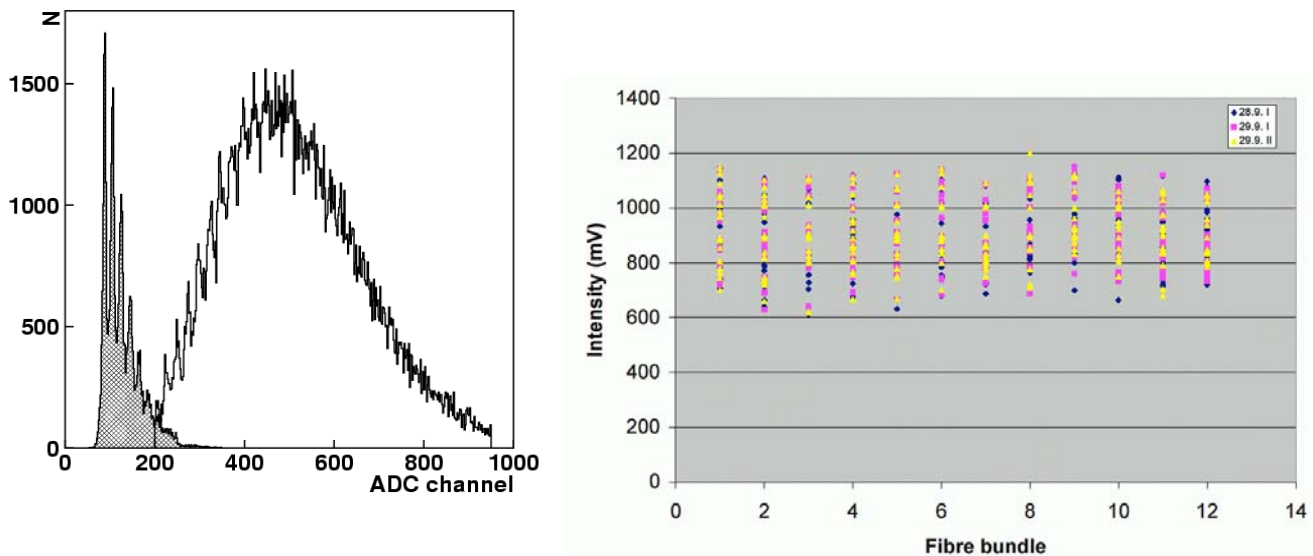Figure 4-7: SiPM pulse height spectrum with single pixel signals.

Figure 4-8: Left: Pulse height spectra for low intensity LED light with MIP signals overlaid. Right: Uniformity of light intensity injected into individual tiles via fibre bundles.

In addition, in order to control the response function of the SiPM, the LED monitoring system is required to deliver light intensities covering the range from few photoelectrons up to 80-100 MIPs. Due to the fast recovery time of the SiPM the duration of the LED pulse must not deviate from that of particle-induced scintillation light (~10 ns), otherwise the response function would change. This puts stringent requirements on the design of the LED driver electronics for which a prototype has successfully been tested (see below). A sensitive preamplifier bridges the gap between the SiPM gain and the PIN diodes coupled with the same type of fibre to the LED as the tiles, such that the same readout can be used. The design is still to be integrated into the calibration and monitoring board (CMB) developed at Prague, which also provides the PIN diodes to monitor the LED amplitude variations as well as communication with DAQ and slow control. A full 12-channel CMB prototype is expected in December 2005.

During the calorimeter operation possible variations in the system are detected by a threefold monitoring system. The slow control system reads the SiPM bias voltage supplied to the baseboard and the temperature of each cassette with 5 sensors. The SiPM gain is measured at the beginning of each run with low LED light intensity. Finally, the peak position of a medium amplitude LED reference signal (PIN diode corrected) is continuously monitored. The total temperature and voltage dependence of the SiPM gain at room temperature is measured to be 1.7%/^{o}C and 2.5%/0.1V, while the signal amplitude varies according of 4.5%/^{o}C and 7%/0.1V, reflecting the additional sensitivity of the photon detection efficiency to temperature and voltage.

4.8   Commissioning in the DESY test beam

The installation of the first module in the DESY electron test beam is shown in Figure 4-9. The slow control and DAQ systems control the movable stage such that the entire surface can be scanned with the beam. The system allows simultaneous gain calibration of all channels (presently limited by the number of LED drivers), MIP and light yield calibration as well as a test of the uniformity for the full cassette, to be extended into the saturation regime with the help of additional absorbers placed upstream of the module such that the tiles are exposed to the shower maximum.
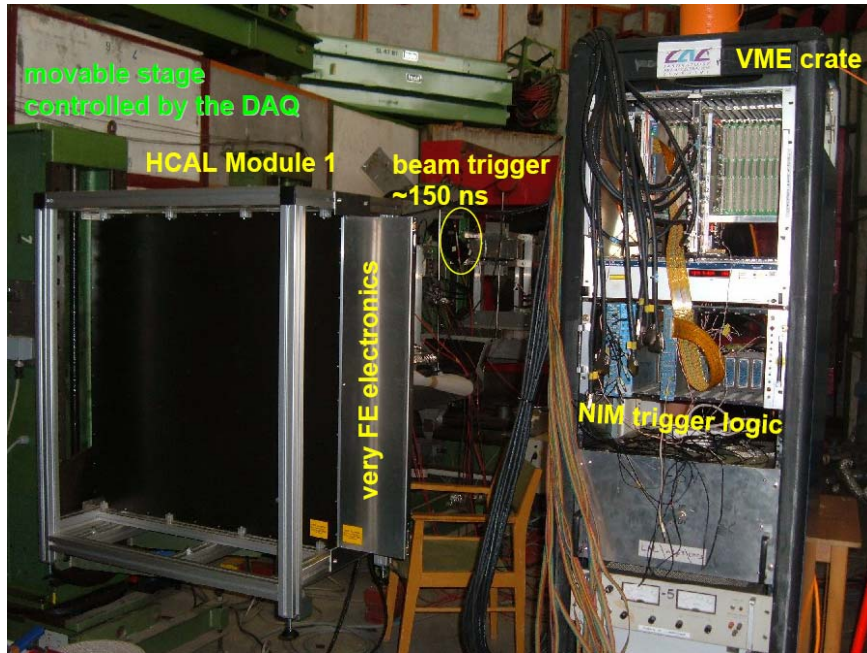
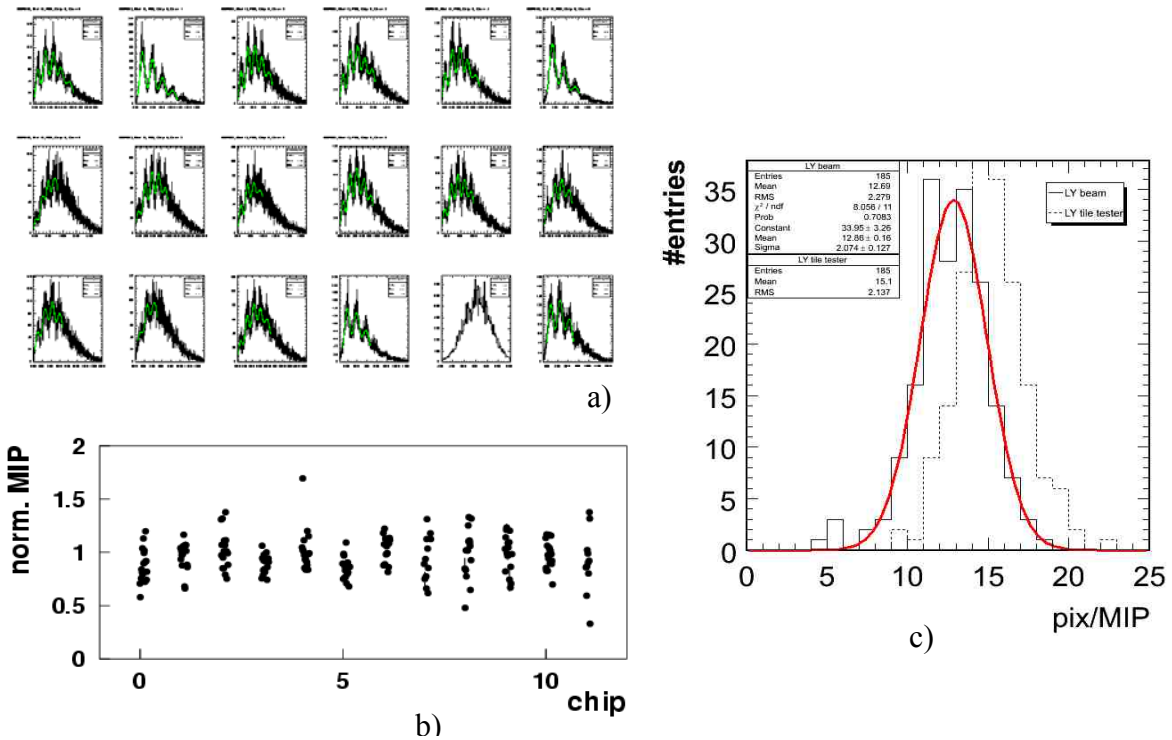Figure 4-9: AHCAL Module ONE in the DESY test beam ("Strahl 22").

Figure 4-10: Spectra for simultaneous gain calibration with low intensity LED light, MIP calibration factors, distribution of light yields measured in the test beam, in comparison with tile test results (obtained at different conditions).

First results from the DESY test beam are shown in Figure 4-10: The low LED intensity spectra for 18 channels connected to one LED are shown in Fig. 9a, with fits used to extract the SiPM gain. The results of the MIP calibration for 197 channels are shown in Fig 9b, they have been shown to be reproducible within 2%. From a combination of the two measurements the distribution of light yields in Fig 9c is obtained. The analysis is in a too early stage to draw quantitative conclusions, but the results are in agreement with expectations. They establish the basic functionality of the readout and calibration components. The tools and the data are in hand for further developing the multi-channel procedures for the commissioning and calibration of the full test beam prototype.

A second set-up with full readout chain is used to establish the monitoring system with cosmic rays and LED signals. Figure 4-11 shows the results from an LED amplitude scan. It demonstrates that a dynamic range sufficient for the control of the non-linearity can be achieved. The light intensity scale is derived from the PIN diode signal, calibrated with the single photon signals of the SiPM. The data points, shown for comparison, have been obtained on a test bench with filters controlling the light intensity.
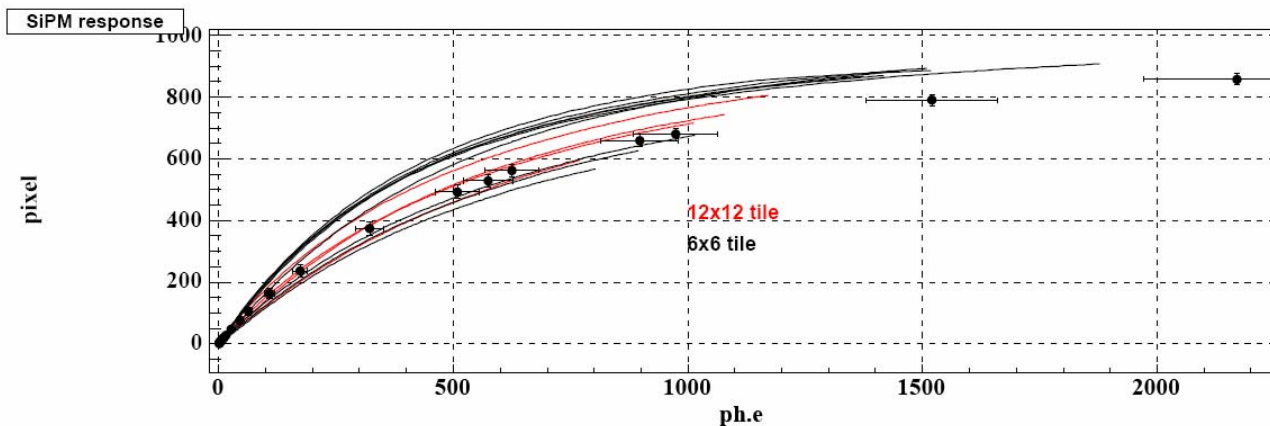

Figure 4-11: SiPM signal in terms of fired pixels vs.light intensity. The curves are obtained with the LED driver prototype mounted on module TWO, using the PIN diode signal as reference. The data points were obtained on a test bench, using filters to control the light intensity

4.9   Conclusion and outlook

The successful operation of the 99-channel "Minical" has established the SiPM as photodetector for calorimetric applications. This opens up new possibilities for highly granular scintillator-based calorimeters. SiPMs are now becoming available in large quantities; a production and quality control chain has been set up and shows reasonably stable sensor properties. Construction and beam commissioning of an 8000 channel calorimeter prototype for combined ECAL and AHCAL hadron beam tests is in progress, using a unified electronic readout concept. The basic functionality of the readout and calibration chain has been verified, and the first multi-channel results are becoming available. Once the SiPM quality control is established, production, test and assembly can proceed with two modules per week. Thus, if all goes well, the system can be ready to collect data in 2006.

In order to proceed from a "proof-of-principle" in the test beam to establishing the scintillator-based HCAL as an option for a detector at the ILC, further R&D will be necessary before technical solutions are in hand which can be scaled to a full detector. Important guidance is expected to come from the final commissioning and test beam operation of the prototype, yet some directions can already be identified:

- The SiPM scintillator technology needs to be further consolidated, including longterm stability and radiation hardness studies.

- SiPMs are under rapid development. With larger active area and/or higher efficiency a further optimized or simplified scintillator-photodetector system would become possible.

- The front-end electronics should incorporate a fast discriminator to auto-trigger the readout. This would decouple shaping times from trigger latency, allowing better exploitation of the fast SiPM response (even for timing purposes) and enhanced calibration capabilities, e.g. by means of radioactive sources. Furthermore, following the R&D lines of the ECAL electronics, the digitization could be integrated in the front end ASIC.

- The electronics cost benefits of the semi-digital approach should be worked out in a realistic design.

- The calibration system might be simplified; test beam experience will show where redundancy might be reduced without loss of operational stability.

- Finally, an integrated electro-mechanical concept for dense layers, avoiding large numbers of cables and connectors, needs to be developed as basis for a mechanical design of the full detector.

This R&D should result in a scalable prototype, corresponding to a sector of the full detector. It needs to be instrumented only partially, sufficient to test channel densities, but it does not have to cover the volume occupied by typical hadron showers. Part of such a programme will benefit from activities within the EUDET initiative.

5   The Tail-Catcher and Muon Tracker (TCMT)

5.1   Overview

The CALICE collaboration is pursuing the construction of a scintillator-steel device which will serve as a tail-catcher and muon tracker [21]. The TCMT prototype will have a fine and a coarse section distinguished by the thickness of the steel absorber plates. The fine section, sitting directly behind the hadron calorimeter and having the same longitudinal segmentation as the HCAL, will provide detailed measurements of the tail-end of the hadron showers which are crucial to the validation of hadronic shower models, since the biggest deviations between models occur in the tails. The following coarse section will serve as a prototype muon system for any design of a Linear Collider Detector (LCD) and will facilitate the studies of muon tracking and identification within the particle flow reconstruction framework. Equally importantly, the TCMT will provide valuable insights into hadronic leakage and punch-through from relatively thin calorimeters (as are being imagined in most LCD designs) and the impact of the coil in correcting for this leakage.

The basic design parameters chosen for the TCMT are as follows:

- 16 layers, each of active area $1{\times}1\text{m}^2$,

- Extruded scintillator strips 5cm wide and 5mm thick,

- Steel absorber with thickness 2cm (8 layers) and 10cm (8 layers),

- X or Y orientation of strips in alternate layers,

- WLS fibre mated to Silicon Photomultiplier (SiPM) photo-detection.

5.2 Fabrication and Assembly

5.2.1 Strip-Fibre System

The extruded scintillator strips are produced at the Scintillator Detector Development Lab (SDDL) extruder facility operated jointly by FNAL and Northern Illinois University (NIU). The extruder uses polystyrene pellets and PPO and POPOP dopants to produce scintillator strips that are 1m long, 10cm wide and 5mm thick and have two co-extruded holes running along their full length. A 1.2mm outer diameter Kuraray wavelength shifting fibre is inserted in each of the holes. Detailed optimization studies of strip-fibre system were carried out to converge on this solution. To have the required 5cm readout segmentation, each of the strips has a 0.9mm wide epoxy-filled separation groove in the middle. All the strips and WLS fibres required for the construction and assembly of the test beam prototype have been fabricated and have undergone rigorous quality control checks (Figure 5-1).
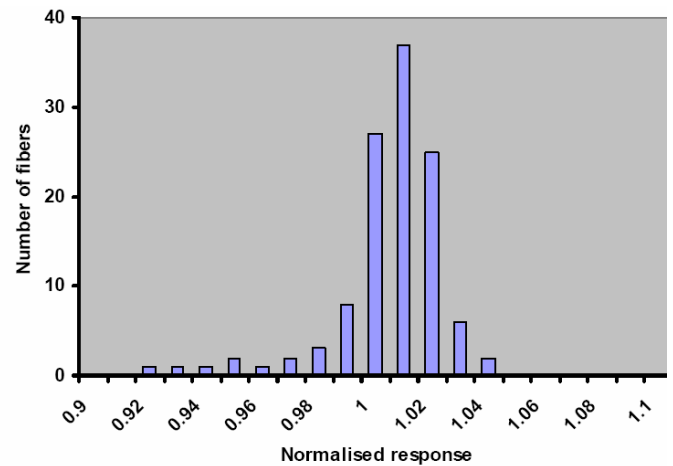

Figure 5-1: Left: Extruded scintillator strips to be used for the TCMT. Right: Normalized response of a set of Kuraray Y11 WLS fibres that will be installed in the TCMT.

5.2.2 Photodetector

The TCMT uses SiPMs for photo-detection. The devices are soldered on to a holder which is in turn mounted close to the strips (Figure 5-2). The fabrication of the holder and its mounting is done with enough precision that the fibre is aligned with the centre of the sensor and close to it (within 150 microns) without touching it. All the SiPM holders required for the device have been fabricated. So far, around 50 SiPMs have been received. All have been soldered to the holders and tested.
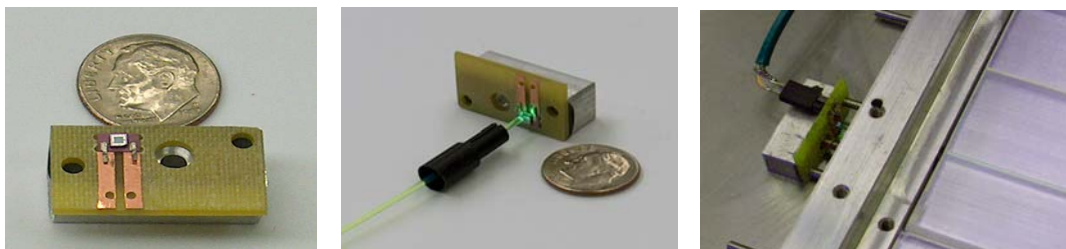

Figure 5-2: The fibre-SiPM interface.

5.2.3   Cassette Assembly

The scintillator strips and their associated photodetectors in each layer will be enclosed in a light-tight sheath which we refer to here as a cassette. The top and bottom skins of the cassette are formed by 1mm thick steel with aluminium bars providing the skeletal rigidity. The aluminium bars also divide the cassette into distinct regions for scintillator, photodetectors, cable routing and LED drivers such that they can be independently accessed for installation, maintenance or repairs. All the cassettes required for the TCMT have been assembled (Figure 5-3). Most of them however do not have photodetector and LED driver boards as these two items are not available in the required quantities at the moment.

Figure 5-3: Assembly of a TCMT cassette.

5.3   Commissioning

One cassette has however, been fully instrumented and has been commissioned with LEDs and cosmic ray muons (Figure 5-4). It has been shipped to DESY for further testing. These tests will initially focus on the integration of this layer into the full electronics readout chain that will be used for the CALICE test beam. One of the practical advantages of using the SiPMs is that, to a large extent, electronics developed at DESY for the AHCAL can be used for the TCMT. This includes, for instance, the preamplifier and DAQ boards. However the different structure and channel count of the TCMT necessitates the development of some intermediate connector and adaptor boards. The design and fabrication of these boards is now complete and the full readout chain is now undergoing tests, as shown in Figure 5-5. It is expected that following the successful integration, the cassette will be exposed to the DESY electron test beam.
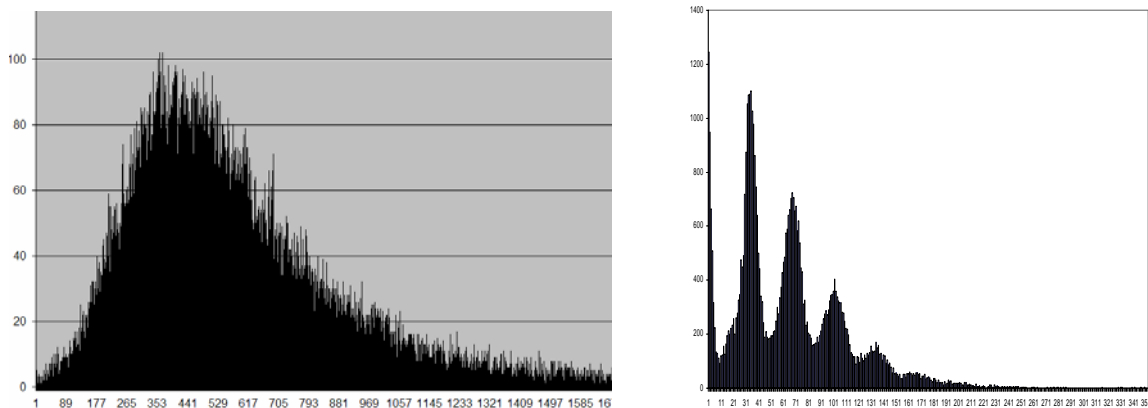

Figure 5-4: Single photo-electron (right) and cosmic spectra (left) for a TCMT cassette channel.
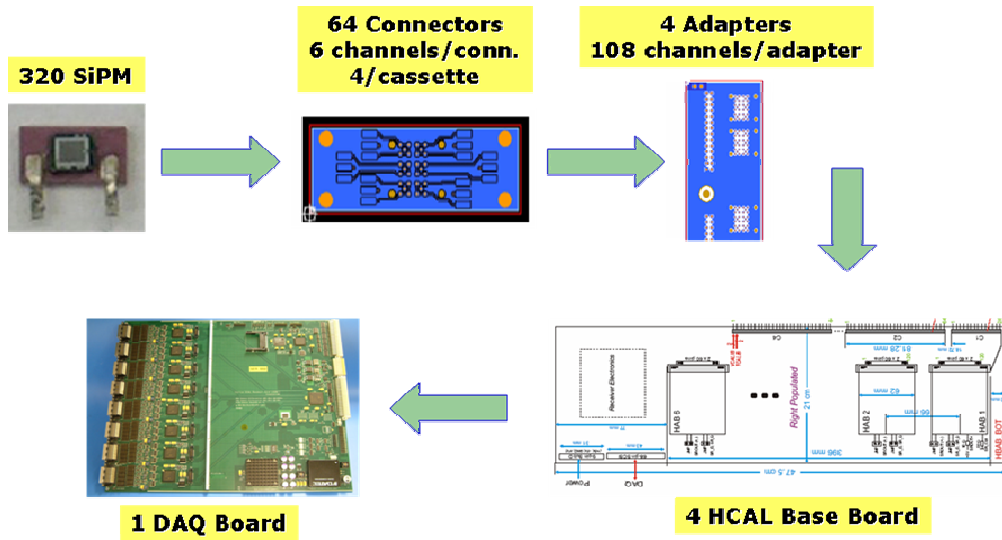
Figure 5-5: Schematic of the TCMT readout chain.

5.4   Absorber Stack and Table

The design of the absorber stack and table is now available (Figure 5-6). The design foresees welding the steel absorber plates to a frame which also doubles as a lifting fixture. The structure will be then placed on top of a table capable of forward-backward and left-right motion. The stack will have the capability of being rotated by 90º for taking normally incident cosmics during beam downtime. The weight of the assembly is approximately 10 tonnes. The absorber plates necessary have already been acquired and the construction of the stack is planned to commence soon.
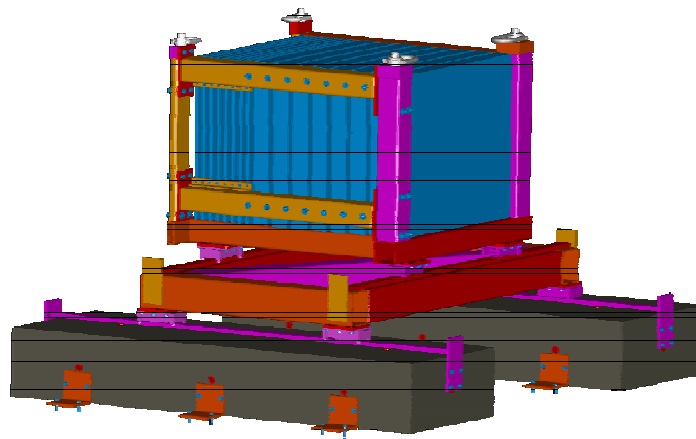

Figure 5-6: The TCMT absorber stack and table.

5.5   Conclusions

The TCMT is well into its construction phase. The construction of the absorber stack and the commissioning of the calibration and slow control system are the next steps on the horizon. However, it is clear that different elements are coming together such that a test beam exposure starting summer to fall of 2006 does not seem unreasonable if the SiPM deliveries are not too delayed.

6   Software

6.1   Overview

There are two principal interconnected strands of software activity within the CALICE collaboration. The first area concerns the overall detector simulation and reconstruction, with particular reference to calorimeter reconstruction and particle flow. The second area of activity is directed towards the preparation for data-taking and of tools for the analysis of test beam data, and the related simulations.

6.2   Detector simulation and reconstruction

The most novel feature of the calorimeters being studied by CALICE is their very high spatial granularity. This is motivated by the need to measure the energies of hadronic jets with unprecedented precision, $O(30\%/\sqrt{E(GeV)})$. There is general agreement that the best way to achieve this is through the "particle flow" approach, in which the energies of charged particles are measured in the tracking chambers, while the energies of photons and neutral hadrons are determined from calorimetry. In order to distinguish these separate energy contributions, highly granular calorimetry with sophisticated pattern recognition software is required. Recent activities in CALICE in this area include the following:

- Two early codes, which indicated the ability of particle flow to achieve the desired resolution, were written by members of CALICE. These were Replic (based largely on work at LLR) which was used for the Tesla TDR, and Snark (written largely at DESY and ITEP), which is embedded in the Brahms reconstruction framework. However, both of these codes are somewhat inflexible and linked to specific detector geometries.

- Recent activities have tended to focus on more general codes, with emphasis on the conceptual detector design studies which were recently initiated as part of the ILC Worldwide Study. The simulation program Mokka [5], based on GEANT4 [6], is central to many of the ILC studies, especially in Europe, and is coordinated by LLR. New features have recently been introduced into Mokka to permit the scaling of detector geometrical parameters such as the radius and length of the calorimeters. These will be essential tools for optimisation studies on the conceptual detector designs.

- A key tool in integrating the various software efforts has been the development of the LCIO "persistency" data format [22], which provides a lightweight common means of communication between various simulation and reconstruction codes. Several CALICE groups, especially DESY and LLR, have been involved in the development of LCIO in collaboration with SLAC. LCIO is now well established as an ILC standard.

- Particle flow studies are continuing in the CALICE groups at Cambridge, DESY, ITEP, Argonne, NIU and UTA, and are regularly reported at CALICE meetings and international ILC workshops. For example, in Figure 6-1 we show results from a recent study of one clustering algorithm, investigating the quality of photon reconstruction in the presence of a nearby $\pi^{\pm}$ and Figure 6-2 shows an example of a reconstructed di-jet mass peak reconstructed with a newly developed realistic particle flow algorithm.
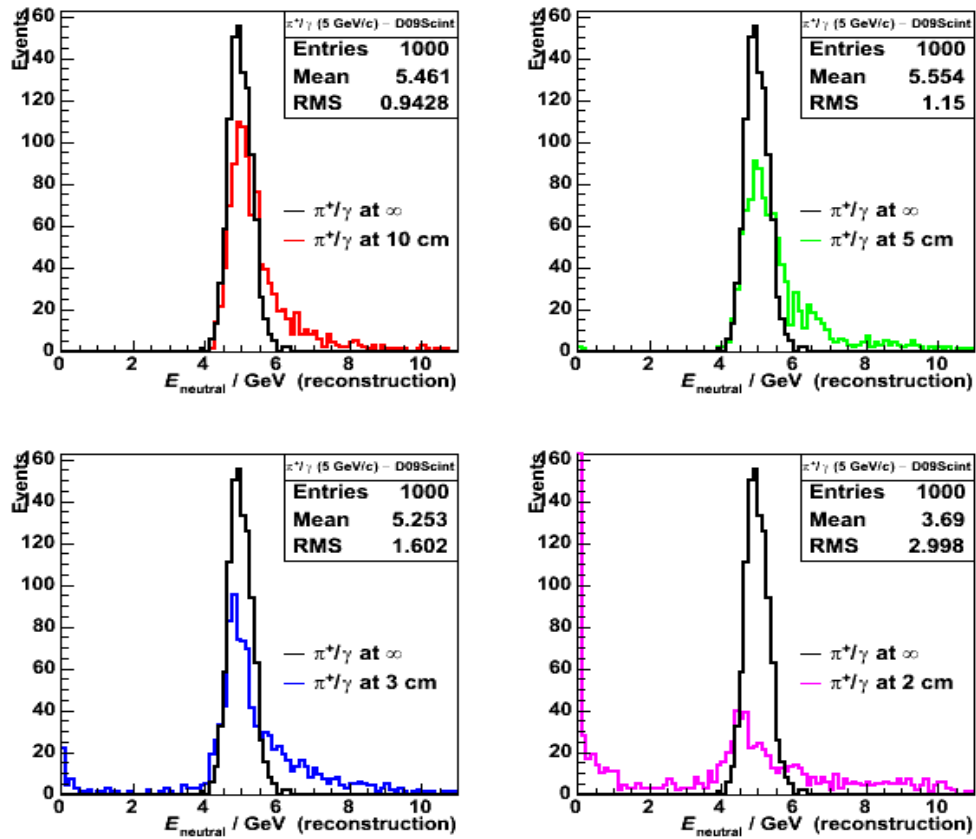
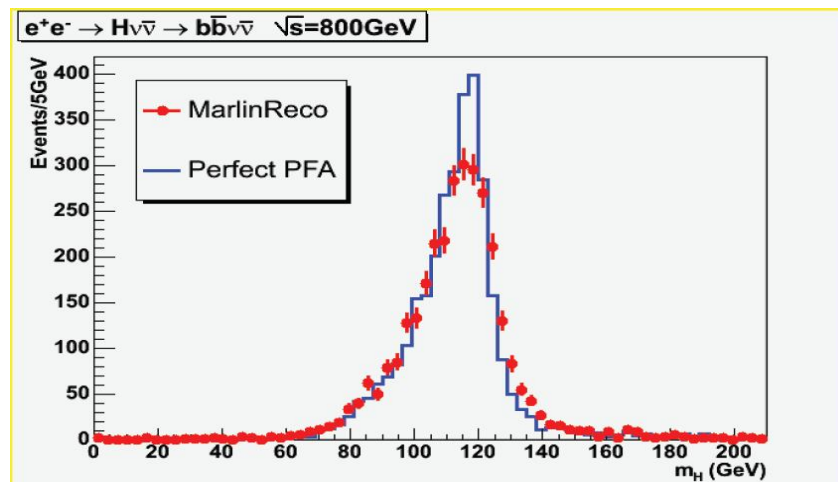Figure 6-1: Photon energy reconstructed in the presence of a nearby pion.

Figure 6-2: Comparison of H→bb mass peak reconstructed with ideal and realistic particle flow.

6.3 Software for the test beam

6.3.1 Online software

The basic requirements for the CALICE data acquisition are to be able to trigger at 1kHz and buffer data for 2000 events during a spill. It should then be able to read out the data and write to disk at a rate of 100Hz.

The software for the online tasks has been implemented in C++/Linux. The code is based on the CERN Hardware Access Library (HAL) code for VME readout and ROOT for graphics, but has no other external dependencies. The requirement of 100Hz readout rate, together with the 50kByte event size, gives a total required rate to disk of 5MBytes/s. Run files are limited to 2GBytes due to Linux file handling downstream, so at full rate, each run is expected to last only seven minutes.

A prototype online software system was used for the cosmics and beam runs earlier in 2005. This had an output raw data file format close to the final system but the online software itself was very preliminary. The rate during the cosmics run was trigger limited and so was not determined by the DAQ system. However, in the beam run, a maximum rate of around 30Hz was achieved, reading 10kBytes per event from the two CRCs used. This only corresponded to a total data rate of around 0.3Mbytes/s.

Work has continued since the beam run to upgrade the system, both in terms of new hardware (mainly much faster PCs) and better software. The current system under development has achieved 130Hz with six CRCs and (by adding faked data corresponding to the other seven CRCs of the final system), a data rate to disk of 6MBytes/s, therefore achieving the requirements. Figure 6-3 shows the time history of the event and data rates a typical test run which lasts around five minutes before reaching the file size limit.

The major remaining issue is the integration of the different subsystems into a coherent DAQ readout. This is scheduled to be done by the end of 2005, when the existing DAQ system together with the ECAL is shipped to DESY.
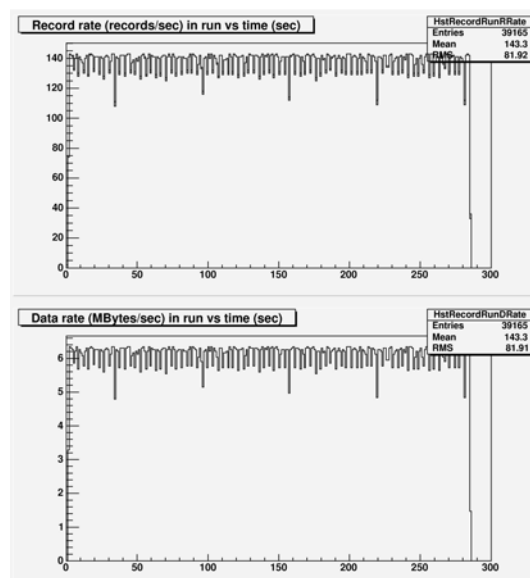
Figure 6-3: Time history and data rate for a typical run

6.3.2   Test beam simulation and analysis software

One key objective of the CALICE test beam program is the validation and testing of the simulation which will be used for the global detector design studies. The Mokka simulation program, in addition to full detector descriptions, includes descriptions of the various CALICE prototypes which are being prepared for test beam studies. Several institutes in CALICE have contributed towards the development of the test beam simulation, including LLR, DESY, NIU, UTA, RHUL and Cambridge.

The test beam setup is implemented into GEANT4 using the Mokka package with a flexible geometry interface. The example shown in Figure 6-4 comprises the drift chambers, the ECAL protoype, the AHCAL prototype and the TCMT. The implementation allows for different impact angles of the primary particles. The CALICE collaboration also maintains a simulation of the test beam setup based on GEANT3 [22] in order to be able to compare with hadronic shower models not available within GEANT4.
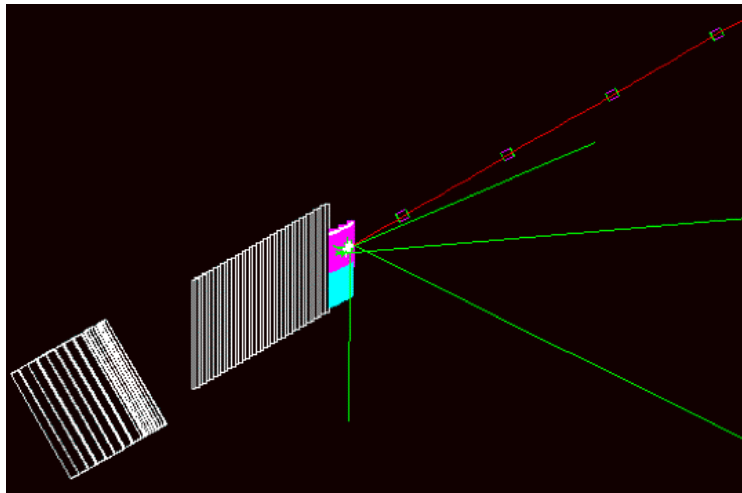

Figure 6-4: Mokka-based GEANT4 implementation of the CALICE test beam setup. Shown are (from right to left) the drift chambers, the ECAL prototype, the AHCAL prototype, and the TCMT.

The test beam activities in CALICE will involve many different groups at different times, and yet it is important to perform a coherent analysis and interpretation of the data. A sizeable volume of data will need to be processed and made accessible to all members of the collaboration. In order to facilitate this, careful consideration has been given to the choice of a suitable lightweight software framework. It was decided to use the same LCIO data format as is already used by the simulation work (both for the test beam and for full detector studies), and which is becoming the *de facto* standard for much ILC work. We intend to perform most of the analysis in the MARLIN [24] framework – a lightweight framework designed originally for ILC simulation analysis work of LCIO events. In this way, members of CALICE can use the same tools for test beam data as they and the rest of the ILC community use for simulation studies.

The data acquisition system delivers the raw data in a special binary format and splits the data into various data types, for example the ADC data representing the energy depositions in the calorimeter cells, TDC data which contain drift chamber information or configuration data which define the trigger setup. The first stage is therefore to convert the raw data from the DAQ into LCIO with minimal processing, and the C++ code for this is now available. The conversion of a typical run of 2GBytes on an Intel Pentium 4 CPU with 2.4 GHz takes roughly 20 minutes and the file size of the resulting LCIO files is roughly 30% smaller than that of the original binary files. All data analyses will start from these LCIO raw data files. The original raw data files are however kept for reference. All data taken during the ECAL test beam at DESY in February 2005 have been converted into LCIO. In addition, the data currently taken with single modules of the AHCAL are converted on a regular basis into LCIO.

The general outline of the analysis chain is indicated in Figure 6-5. In order to store and share data such as calibrations and trigger configuration, a database is needed. A package LCCD (Linear Collider Conditions Data) [25], which stores LCIO objects in a MySQL database, and can be conveniently used in Marlin, has been adopted. A master database is set up at DESY, which is accessible from all interested CALICE institutes.
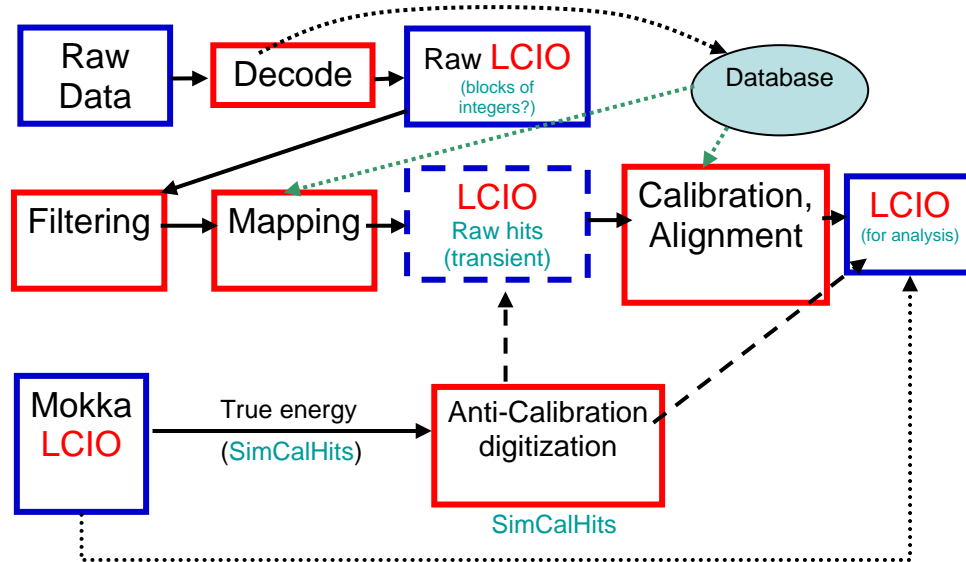
Figure 6-5: Outline of the reconstruction data flow for test beam data and simulation.

Roughly 250 GByte of raw data were collected during a three week period at the DESY test beam with the first version of the protoype of the electromagnetic calorimeter. The data are centrally stored in the DESY dCache pool. The complete test beam program will produce a data volume of the order of 3-5 TBytes which will be stored in the same location. The data can be automatically copied into the dCache pool when a data run has been finished and are immediately accessible using grid tools.

Conditions data denote all kinds of data which are needed to analyze the data beside the actual event data, e.g. calibration constants or the mapping between the hardware addresses and physical detector cells. The conditions data needed for the CALICE test beam effort are kept in a MySQL database which is centrally hosted by DESY and made available to the CALICE collaboration via network access. The software package CondDBMySQL [26] provides a convenient interface to a MySQL database and allows for the definition of validity ranges of the conditions data in terms of time stamps. The need for the maintenance of conditions data within the CALICE test beam measurements motivated the development of the LCCD software package. It allows the storage of conditions data in various formats such as simple files, information attached within LCIO to an LCEvent or a MySQL database. The LCCD package establishes an interface to CondDBMySQL which is compatible with the interface to other sources of conditions data.

Processors to calibrate the data have already been developed. LCIO Files containing calibrated hits from the data, suitable for comparison with simulation can be written out for further analysis. These data may be input to e.g. Marlin processors which have been developed for cluster reconstruction for global ILC detector studies but which are flexible enough to be applied in the analysis of test beam data, too. Figure 6-6 shows an example of a comparison between data and simulation performed using the full LCIO-Marlin framework described above.
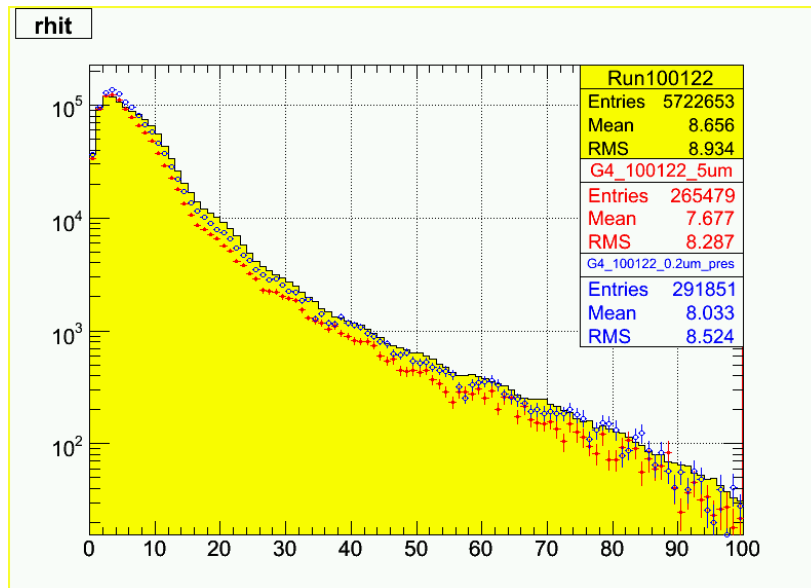
Figure 6-6: Comparison between test beam data (solid histogram) and two simulations (points with errors). The quantity plotted is the radial distribution of energy in 1 GeV electron showers (in cm). The red points correspond to default GEANT4, the blue points correspond to GEANT4 with the step range cut reduced.

7   Test Beam Requirements

The main goal of the test beam is to study the details of the hadronic shower development to the extent that is required for topological reconstruction and accurate simulation of their structure. Large data samples will be needed for this purpose. In order to obtain a quantitative estimate of the precision necessary to test the simulation models, test beam data simulated with the GEANT3 and the GEANT4 programs have been compared. Differences are clearly visible in samples of 10k events, and they depend on energy, particle type (pion or proton) and active detector material. Taking variations of impact point and incidence angle into account, one arrives at data sets of the order of 10^8 events, which require a few weeks of beam time with a DAQ system capable of taking events at 100Hz. To allow for feedback from analysis, several such periods will be needed.

In order to match the typical particle energies in linear collider events, the energy range of the test beam should extend at least up to 50 GeV, but availability of low energies close to 1 GeV is equally important to accurately model the lower energy particles in hadronic jets. Different particle types (pions, protons, and muons) are needed, with high purity (from particle identification devices, e.g. Cherenkov counters) or at least with an accurately known composition. A tracking system must provide the impact point with at least 1mm precision. Other requirements, such as on infrastructure, have been formulated in a document published by the worldwide LC test beam group.

A test of the fully equipped ECAL is expected during the first months of 2006 at DESY. The goal is to quantitatively test the ECAL data versus the GEANT4 simulation.

The collaboration is preparing a MoU to be sent to CERN-SPSC, requesting a period of running with our ECAL and AHCAL prototypes on ones of the test beam (H2, H4, H6 or H8). The electron beam purity, the spill structure, and the energy range on this test beam area are well suited for standalone ECAL tests, which is foreseen initially. When the AHCAL prototype is ready later in 2006, we will have a substantial data-taking period using a wide range of energies, particle types, incident angles, etc. This test will include the TCMT.

At the beginning of 2007, we hope to move to the Meson Test Beam Facility (MTBF) at FNAL, where a space is available for our test with a hadron beam. Optimising the beam structure and beam quality (purity, energy range, etc.) is under discussion with FNAL Directorate. Tests here will be done with the ECAL and both the AHCAL and DCHAL, including any layers of GEM detectors which become available, as well as the TCMT.

8   <u>Conclusions</u>

The collaboration, enlarged with new groups, remains mainly focussed on the test beam goal. Taking into account the information given above, the collaboration proposes to proceed further, asking for a period of three months of test beam in DESY starting at the beginning of February 2005 with the ECAL fully-equipped in depth. It is intended that this will be followed by a period of test beam at CERN for the ECAL and AHCAL. Following this, the major data period with all prototypes at FNAL is intended for 2007.

We ask the PRC to recommend the use of the DESY test beam in 2006 and endorse our goals over the coming years.

9   <u>References</u>

[1]   J.Fleury [CALICE Collaboration], "Front end electronics for a Si-W calorimeter", LCWS04, Paris, 2004.

[2]   P.D.Dauncey [CALICE Collaboration], arXiv:hep-ex/0410001; M.Warren, "The CALICE Electromagnetic Calorimeter Readout Electronics", presented at IEEE Nucl. Sci. Symp., Rome, October 2004.

[3]   F.Sauli, Nucl. Inst. Meth. **A386**, 531 (1997).

[4]   ALEPH Collaboration, Nucl. Inst. Meth. **A360**, 481 (1995).

[5]   Mokka Home Page, http://polywww.in2p3.fr/GEANT4/tesla/www/mokka/mokka.html.

[6]   GEANT4, S.Agostinelli, *et al.*, "GEANT4 - A simulation toolkit", Nucl. Inst. Meth. **A506**, 250 (2003), http://GEANT4.web.cern.ch/GEANT4/.

[7]   F.Richard, *et al.*, "TeV Energy Superconducting Linear Accelerator (TESLA) Technical Design Report", (2001); http://tesla.desy.de/new_pages/TDR_CD/start.html.

[8]   S.Habib, "Simulation Studies of a New Digital Hadron Calorimeter, Using Gas Electron Multipliers (GEM)", MSc Thesis, University of Texas at Arlington, UTA-HEP/LC-003, Unpublished (2003).

[9]   V.Kaushik, "Performance of Novel Digital Hadron Calorimeter Using Gas Electron Multiplier (GEM) and the Energy Flow Algorithm Development," MSc Thesis, University of Texas at Arlington, UTA-HEP/LC-004, Unpublished (2004).

[10]   J.C.Brient, J.Yu, eds, World-wide Linear Collider Test Beam Working Group, "International Linear Collider Calorimeter Test Beam Program (A Planning Document for Use of Test Beam Facility at FNAL)," FNAL-TM-2291, In preparation (2005).

[11]   F.Sefkow [CALICE Collaboration], LC-DET-2004-022 Prepared for 11th International Conference on Calorimetry in High-Energy Physics (Calor 2004), Perugia, Italy, 28 Mar - 2 Apr 2004.

[12]   G.Mavromanolakis and D.R.Ward, arXiv:physics/0409040.

[13]   V.Morgunov and A.Raspereza, arXiv:physics/0412108.

[14]   A.Dyshkant *et al.*, IEEE Trans. Nucl. Sci. **51**, 1590 (2004).

[15]   E.Garutti [CALICE Collaboration], proceedings of the International Linear Collider Workshop 2005, Stanford, USA; V.Korbel and V.Morgunov, LC-DET-2001-051.

[16]   R.Poeschl [CALICE Collaboration], proceedings of the International Linear Collider Workshop 2005, Stanford, USA.

[17]   P.Buzhan et al., Nucl. Inst. Meth. **A504**, 48 (2003).

[18]   V.Andreev et al., Nucl. Inst. Meth. **A540**, 368 (2005); V.Korbel, LC-DET-2004-028.

[19]   J.Cvach [CALICE Collaboration], proceedings of the International Linear Collider Workshop 2005, Stanford, USA.

[20]   G.Martin-Chassard [CALICE Collaboration], proceedings of the International Linear Collider Workshop 2005, Stanford, USA.

[21]   D.Chakraborty [CALICE Collaboration], proceedings of the International Linear Collider Workshop 2005, Stanford, USA.

[22]   F.Gaede *et al*., "LCIO - A persistency framework for linear collider simulation studies", LC-TOOL-2003-053.

[23]   R.Brun *et al*., GEANT3.21 program.

[24]   F.Gaede *et al.,* MARLIN, http://ilcsoft.desy.de/marlin

[25]   F.Gaede, "Overview of Simulation and Reconstruction Tools in Europe", http://ilcsoft.desy.de/lccd

[26]   For a reference see http://savannah.cern.ch/projects/conddb-mysql